



UNIVERSITY OF LEEDS

This is a repository copy of *Single point incremental forming: An assessment of the progress and technology trends from 2005 to 2015*.

White Rose Research Online URL for this paper:
<http://eprints.whiterose.ac.uk/115901/>

Version: Accepted Version

Article:

Behera, AK orcid.org/0000-0002-1058-5335, de Sousa, RA, Ingarao, G et al. (1 more author) (2017) Single point incremental forming: An assessment of the progress and technology trends from 2005 to 2015. *Journal of Manufacturing Processes*, 27. pp. 37-62. ISSN 1526-6125

<https://doi.org/10.1016/j.jmapro.2017.03.014>

© 2017 The Society of Manufacturing Engineers. Published by Elsevier Ltd. This manuscript version is made available under the CC-BY-NC-ND 4.0 license
<http://creativecommons.org/licenses/by-nc-nd/4.0/>

Reuse

Items deposited in White Rose Research Online are protected by copyright, with all rights reserved unless indicated otherwise. They may be downloaded and/or printed for private study, or other acts as permitted by national copyright laws. The publisher or other rights holders may allow further reproduction and re-use of the full text version. This is indicated by the licence information on the White Rose Research Online record for the item.

Takedown

If you consider content in White Rose Research Online to be in breach of UK law, please notify us by emailing eprints@whiterose.ac.uk including the URL of the record and the reason for the withdrawal request.



eprints@whiterose.ac.uk
<https://eprints.whiterose.ac.uk/>

Single Point Incremental Forming: An assessment of the progress and technology trends from 2005 to 2015

Amar Kumar Behera^{1,a}, Ricardo Alves de Sousa^{2,b}, Giuseppe Ingarao^{3,c},
Valentin Oleksik^{4,d}

¹School of Mechanical Engineering, University of Leeds, Woodhouse Lane, Leeds, LS2 9JT, UK

²Department of Mechanical Engineering, University of Aveiro, Campus de Santiago 3810-183 Aveiro – Portugal

³Department of Industrial and Digital Innovation, University of Palermo, Viale delle Scienze, 90128 Palermo, Italy

⁴Department of Industrial Machinery and Equipment, Lucian Blaga University of Sibiu, 10 Victoriei Bd, Sibiu 550024, Romania

Emails: ^aa.k.behera@leeds.ac.uk, ^brsousa@ua.pt, ^cgiuseppe.ingarao@unipa.it, ^dvalentin.oleksik@ulbsibiu.ro

Abstract.

The last decade has seen considerable interest in flexible forming processes. Among the upcoming flexible forming techniques, one that has captured a lot of interest is Single Point Incremental Forming (SPIF), where a flat sheet is incrementally deformed into a desired shape by the action of a tool that follows a defined toolpath conforming to the final part geometry. Research on SPIF in the last ten years has focused on defining the limits of this process, understanding the deformation mechanics and material behavior and extending the process limits using various strategies. This paper captures the developments that have taken place over the last decade in academia and industry to highlight the current state of the art in this field. The use of different hardware platforms, forming mechanics, failure mechanism, estimation of forces, use of toolpath and tooling strategies, development of process planning tools, simulation of the process, aspects of sustainable manufacture and current and future applications are individually tracked to outline the current state of this process and provide a roadmap for future work on this process.

Keywords: incremental forming; geometric accuracy; formability; process limits; technology assessment; applications

1. Introduction

Rapid advances in the use of computers in sheet metal manufacturing processes has led to several novel flexible forming processes that have evolved from conventional techniques. One of these upcoming processes is Single Point Incremental Forming (SPIF). SPIF is a sheet metal part manufacturing process in which a part is formed in a stepwise manner incrementally by a CNC controlled tool, which is usually hemispherical in shape [1], as illustrated in the schematic shown in Fig. 1. The process provides a degree of flexibility higher than other forming processes as it does not require a dedicated die to operate. This, in turn, results in reduced lead-time and cost of tooling. As a result, it helps in relatively fast and cheap production of small series of sheet metal parts. On the other hand, the process itself is quite slow compared to traditional forming processes such as stamping and deep drawing, lacks the ability to form steep wall angle parts in a single pass and is faced with limited forming limits and dimensional accuracy.

Incremental forming has evolved from a mere technical idea without a real implementation, as illustrated in a patent by Leszak [2] to several different implementations in hardware and software in different research laboratories and industry. The basics of the process in terms of hardware configurations, process limits and achievable accuracy were discussed in a 2005 CIRP keynote paper [3]. Subsequently, the research work in this field has expanded to include improved hardware that enable forming with higher process limits [4, 5], better understanding of the deformation mechanism [6, 7], faster numerical simulation techniques for prediction of forces [8], failure and accuracy [9], improved dimensional accuracy in parts [10-12], new

commercial applications [13], and computer aided process planning tools in the form of software packages with advanced algorithms enabling higher levels of automation [14, 15]. In addition, the use of materials in this process has expanded from metallic alloys to include polymers [16, 17], composite panels [18] and shape memory alloys [19], thereby enabling new application areas for this process. Advances in dimensional metrology and computer aided design tools have led to better quality control of the process [10, 20].

While there has been a lot of research into this process over the years, there is currently a lack of standardization in the approaches taken to realize optimized part manufacture. Although the field has been reviewed in recent times [21-25], these efforts have been limited in scope primarily looking at specific aspects and factors of influence that have been explored by research groups at a single research unit. For instance, the review of Emmens et al. [25] is a historical review covering patents in the field primarily. Hence, it has limited applicability for experimental researchers working on the process. Likewise, the review of Ou et al. [22] covers process parameters while the work of Jeswiet et al. [21] is primarily targeted at reporting some new experimental research output rather than a full scale review of the process. Hence, there is a need to establish benchmarks that will enable the full scale industrialization of this process. With a view to achieving this objective, this paper tries to capture and harmonize the developments that have taken place in this process over the last 10 years with the objective of laying out a condensed representation of the current state of the art covering all aspects in this field that can thereby throw light on the future developments that can take place using this manufacturing process. The paper is structured to cover the basics and requirements for the process in the next two sections in terms of hardware, forming mechanics, forces and toolpath strategies. This is followed by two sections that cover in detail the efforts made to overcome the limitations of SPIF, viz.: process limits and accuracy. Next, the efforts to model the process are covered followed by a section on efforts to make the process sustainable. Finally, the application areas of SPIF are discussed to bring forth the current and future areas of commercial exploitation.

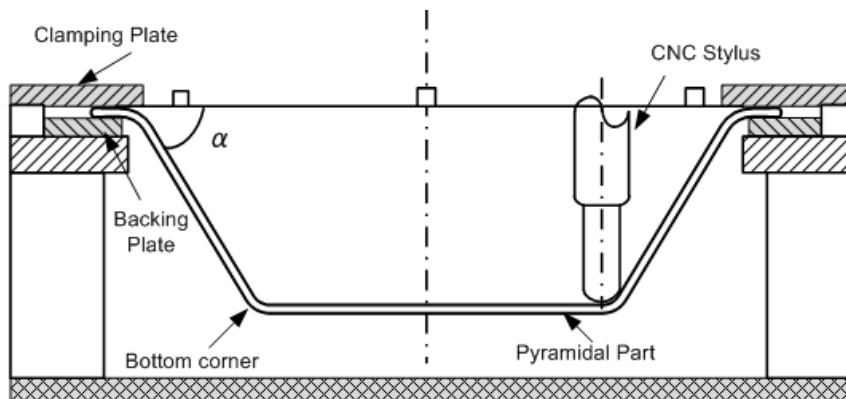


Fig.1. Schematic of Single Point Incremental Forming (SPIF) used to form a truncated pyramid from a flat blank using a CNC style with a hemi-spherical end with a slope α ; a backing plate corresponding to the top contour of the geometry being formed is typically used to support the part close to the top while clamping plate clamp the sheet to the rig used for SPIF [12] [with permission from publisher]

2. Hardware Requirements

One of the key characteristics of the incremental forming process is that it is a slow process compared to traditional sheet forming operations such as stamping. Hence, a key technological requirement for industrial mass manufacture is to speed up the process to make it a competitive solution. However, high feed rates come with their own trade-offs and the design requirements for such machines change. The requirements for nominal feed rates less than 2 m/min. and high feed rates are discussed separately next.

2.1 Requirements for nominal feed rates

A number of considerations need to be taken into account to select a good setup for incremental forming. Several parameters such as the maximum payload (carrying capacity defined by the weight the machine tool or robot can lift), toolpath flexibility, stiffness and overall cost as some of the key decision variables have been identified in designing an optimal setup [4, 26]. Three categories of machines are typically used for

incremental forming, viz.: adapted milling machines, robots and special purpose machines [4]. Of these, milling machines are generally stiffer (typically ~ 200 kN/mm) compared to the robots (typically ~ 0.1 -120 kN/mm) with the result that the accuracy is higher in making parts with milling machines [27, 28]. However, most industrial robots come with a larger working range, making them more suitable for large-sized parts. Other than these, different research groups have attempted building special-purpose incremental forming setups, as in Cambridge [29], Aveiro [4] and the Amino Corporation of Japan [30]. The setup at Cambridge used a passive tool that can rotate freely allowing for exchange of tool tips using bearings for thrust and rotation in close proximity to the workpiece within a support providing high stiffness. The workpiece was mounted on a load-cells based structure with 6 DOFs avoiding moment loads on the cells. The purpose built machine in Aveiro [4] introduced a Stewart platform adaptation, allowing six independent degrees of freedom.

Equipment intended for SPIF covers different topologies of machines used in the industry and in academic research. Fig. 2 illustrates representative setups from different research groups. The execution of the SPIF process presents a few essential aspects: it uses a simple spherical tip to build different shapes and the main process feature is the numerical control of the tool axis. The axis control depends on the degrees of freedom (DOF) available on the machine. The most common applications to perform SPIF experiments have been carried out using an adapted CNC milling machine. Their advantages are the ease of upgrade to work as SPIF machine, high stiffness and productivity rate. On the other hand, it offers a limited number of DOF [3].

The industrial robotic arm has been chosen as an alternative by several research groups [31-35]. The added flexibility given by the available six axes allows the tool positioning at different angles relatively to the sheet surface and gives the possibility to combine multiple steps with a single tool. The robotic arm has a large working volume and fast operation. The major drawbacks are the low stiffness and a very low maximum force, which leads to a less accurate tool position, especially under high loading conditions [3].

2.2 Requirements for high feed rates

Attempts have also been made to carry out high feed rate incremental forming. Ambrogio et al. [36] and Vanhove et al. [37] used CNC lathes to carry out SPIF at feeds less than 600 m/min., which is two orders of magnitude higher than conventionally done. Ambrogio et al. [36] used a Mazak™ Q-Turn 1000 CNC lathe to form pure titanium and TiAl6V4 and found that while the grain size increases due to elevated temperatures, the microstructure of these alloys did not change and concluded that high feed rate SPIF could be performed. Vanhove et al. [37] formed an aluminium alloy, AA 5182-O at feeds up to 600 m/min. and recorded the forces and temperatures during the process. They found that high feeds had a positive effect on ductile behaviour at room temperature and increased the maximum forming angle to 65° . Hamilton and Jeswiet [38] studied the effects of increasing the feed rate to 8.89 m/min., particularly looking into surface roughness and recommended that using specific speed (defined as spindle speed/feed rate) and shape forming factors (defined as forming angle/tool diameter), surface roughness can be controlled. In particular, they looked deeply into the “orange peel” effect, which is the development of a roughened look on the side of sheet that is not in contact with the tool and found limits of forming before this effect occurs. Likewise, Bastos et al. [39] looked at high feed rate forming of one grade of aluminium, AA1050-H111 and three grades of dual-phase steel, DP600, DP780 and DP1000 using the Stewart platform based SPIF-A set up and found that formability and surface finish deteriorated on increasing feed rates for the steels with little effect on the formability of the aluminium alloy.

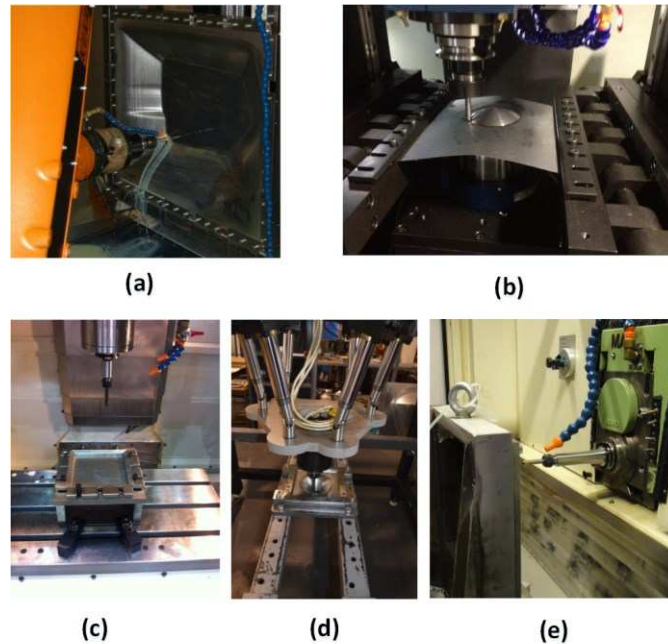


Fig.2. Different hardware setups for incremental forming: (a) KUKA robot [40] (b) forming on a die with sheet clamped on two sides and free on two [20] (c) milling machine with a vertical spindle [14] (d) Stewart platform [4] (e) MAHO 600C milling machine with a horizontal spindle[with permission from publishers]

2.3 End effectors

End effectors for SPIF can be of varying types depending on tool material, coating, diameter and geometric shape. The tool material and coating affect the forming forces and surface roughness of the formed parts. Forming with an acetal tool was found to result in higher surface roughness but with a more isotropic finish as compared to a carbide tool [41]. Based on geometric shape, tools can be classified as hemispherical, ball bearing and flat end, although other shapes exist [42]. Flat end tools have been found to result in better profile accuracy and formability compared with hemispherical tools [42]. The tool diameter affects the scallop height and consequently, the surface roughness of the formed parts [43]. Jeswiet et al. note that higher forming angles may be realized by lowering the tool diameter [21]. However, with a lower tool diameter, more number of passes are required to form the part, thereby increasing the forming time. Besides, the tool must have adequate strength to form the sheet, and this in turn, requires the diameter to be large enough to guarantee this. Typically, the tool diameter varies between 5 and 100 mm, more preferably between 6 and 50 mm and most preferably between 8 and 15 mm [44].

2.4 Technology assessment and future guidelines

To meet the demands of formed parts across length scales, the process capabilities of incremental forming will need to encompass hardware that can support both miniature parts forming at the micro-scale and large parts that exceed the current capabilities of research setups. This will need additional process investigation at these length scales and developing the machine tools that can support such dimensional variations. While current robotic setups address the issues of forming large sized parts to a certain extent, stiffness remains a concern on such setups, preventing the forming of accurate enough parts for industrial valorization. Again, investigations at the micro-scale have been limited, such as the forming of thin aluminium foils by Obikawa et al. [45, 46]. Research on the effects of varying end effectors and controlling the forming forces by altering end-effector designs have been limited [47] and can provide a step change in the achieved surface finish and dimensional accuracy of formed parts. Furthermore, the incorporation of multi-axes spindles into SPIF setups using the next generation of machine tools can help enhance process limits and ability to form more complex parts than currently achieved.

3. Process fundamentals

3.1 Forming mechanics and formability.

The formability of incremental forming is higher than that of conventional forming processes such as stamping [48]. The points on the forming limit curve lying on the right hand side of the forming limit diagram form a negative slope, as illustrated in Fig. 3. Jeswiet et al. [48] observed that the forming limits can be characterized by the maximum wall angle before failure occurs. This maximum angle is dependent on the material type, sheet thickness and process parameters such as tool radius, step down, feed rate, local temperature of the sheet etc. [43]. Typically, two types of parts are used to determine this angle: i) constant wall angle parts such as a cone or ii) variable wall angle parts such as a hyperboloid cup. A list of such wall angles for different materials is provided in Table 1. However, for parts with varying wall angle, the failure wall angle will depend on the geometric shape being formed and may exceed the estimate obtained by constant wall angle parts by $\sim 4^\circ$, as shown by Hussain et al. [49].

Filice et al. [50] did experiments to find out if online monitoring of the tool force could be used for predicting failure. By using this technique, they were able to prevent failure in a conical part, by observing the force trend and changing the process parameters (tool diameter and step down). The later force models of Aerens et al. [51] support this selection of process parameters, where the axial force is proportional to the step down and tool diameter. Szekeres et al. [52] showed that while on-line monitoring was useful for conical parts, it would not help for pyramidal parts. This was because for pyramids, ribs separating the planar faces acted as reinforcements and thereby masked any potential force increase just prior to failure. Hussain et al. [53] derived empirical forming limit diagrams where the reduction in cross-sectional area at tensile failure was used as a criterion for determining failure in SPIF. Eyckens [54] explains why conventional forming limits diagrams fail for SPIF. The reasons ascribed are that conventional FLCs are valid only under the assumptions of linear strain path, negligible through thickness shear, plane stress and deformation caused primarily by membrane forces with no bending. These conditions are not met in incremental forming. Centeno et al. [55] carried out failure limit studies on AISI 304 found that a postponed necking followed by ductile fracture was the responsible mechanism, especially for higher tool diameters giving a low ratio (t_0/R) of the initial sheet thickness (t_0) to the tool radius (R). The failure limits were dependent on the tool diameter and reducing the diameter enhanced formability. A comparison with stretch bending revealed that while in stretch bending, the fracture strains were located close to the fracture forming line, in SPIF, they were much above.

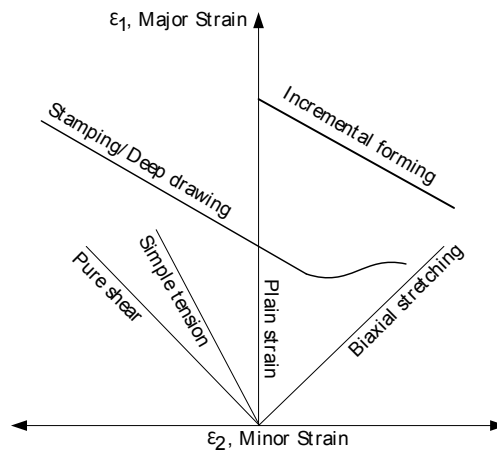


Fig.3. Schematic representation of FLC in SPIF compared with conventional forming [56] [with permission from publisher]

Several analytical and experimental methods and numerical modeling techniques have been used to explain formability in SPIF. Emmens and Van den Boogaard [57] tried to examine whether the forming mechanics in incremental forming could be explained by forming by shear. Later, in 2009, the mechanisms to explain improved formability in SPIF have been outlined in detailed by the same authors [58], who have summed up the different explanations as six different phenomena: contact stress; bending-under-tension; shear; cyclic straining; geometrical inability to grow and hydrostatic stress. While the first five have been able to explain

localized deformation in SPIF, the last one fails to explain the higher location of the FLC but may explain the evolution of voids and fracture limit. Prior to this work, Silva et al. [59] proposed a closed form theoretical model for rotational symmetric SPIF that was built by carrying out membrane analysis with bi-directional in-plane contact friction forces. Using this model, cracks in SPIF of rotationally symmetric parts are claimed to be caused by meridional tensile stresses and not by inplane shearing stresses. In building this model however, strain hardening and anisotropy effects were not taken into consideration while bending effects were only indirectly included in the analysis.

Table 1. Maximum achievable wall angle for different materials

Material	Formed specimen geometry	Tool diameter (mm)	Thickness (mm)	Max. achievable wall angle	Source
65Cr2	Truncated cone	10	0.5	57°	[43]
AA 1050-O	Truncated cone	10	1.5	76°	[60]
AA 2024-T3	Truncated cone	10	1.0	42°	[43]
AA 3003-O	Truncated cone	10	0.85	70°	[43]
AA 3003-O	Truncated cone	10	1.2	71°	[43]
AA 3003-O	Truncated cone	10	2	76°	[43]
AA 3103	Truncated cone	10	1.5	75°	[43]
AA 5086-H111	Truncated cone	10	0.8	62°	[43]
AA 5182	Truncated cone	10	1.25	64°	[43]
AA 5182	Truncated cone	25.4	0.93	63°	[48]
AA 5754 (AlMg3)	Truncated cone	10	1	64°	[60]
AA 5754 (AlMg3)	Truncated cone	10	1.5	71°	[43]
AA 6111-T4P	Truncated cone	25.4	0.93	53°	[48]
AA 6114-T4	Truncated cone	12	1.0	60°	[3, 61]
AISI 304	Truncated cone	10	0.4	63°	[60]
Brass	Truncated cone	12	1	40°	[3, 61]
Copper	Truncated cone	12	1	65°	[3, 61]
DC01	Truncated cone	10	1	67°	[60]
DC04	Truncated cone	10	1	64°	[43]
DDQ	Truncated cone	12	1	70°	[3, 61]
DP600	Varying wall angle conical frustum	16	1	68°	[39]
DP780	Varying wall angle conical frustum	16	1	45°	[39]
DP1000	Varying wall angle conical frustum	16	1	39°	[39]
HSS	Truncated cone	12	1	65°	[3, 61]
Ti grade 2	Truncated cone	10	0.5	47°	[43]
TiAl6V4	Truncated cone	10	0.6	32°	[43]
Polyamide	Varying wall angle conical frustum	10, 15	2, 3	75.4°*	[16]
Polyvinyl chloride	Varying wall angle conical frustum	10, 15	2, 3	75.4°*	[16]
Polyethylene	Varying wall angle conical frustum	10, 15	2, 3	81°**	[16]

* - This is an average over tests with varying tool diameter, sheet thickness and initial drawing angle

** - This is a peak over tests with varying tool diameter, sheet thickness and initial drawing angle

Using the same fundamentals, Martins et al. [62] analysed the enhanced formability of SPIF by combining membrane analysis with ductile damage mechanics. They have provided an explanation by using fracture forming limit diagrams based on the onset of fracture instead of the conventional forming limit diagrams based on the onset of necking. In later work, Fang et al. [7] developed an analytical approach to describe the localised deformation mechanism. In their work, they assumed a plane strain condition in the analytical model, which take into account the material deformation in the plane perpendicular to the tool motion direction. The localised deformation region was divided into sub deformation regions: i) the contact area between the tool and the sheet, and ii) the wall of the formed part in the neighbourhood of the first region. In each one, the state of stress and strain was analysed through the thickness direction to include the bending effect. In addition, stretching effects were also considered by calculating the thickness strain and, finally, the strain hardening was assessed. The results confirmed the accuracy of the analytical model using both finite element simulation and experiments. Experimental validation was performed by measuring the circumferential and meridional strain variations, growth of crack and morphological analysis of the fractured region. The measured meridional strain was larger than the circumferential strain, which confirmed the plane strain assumption used in the analytical modelling. The analytical evaluation revealed that the deformation occurred not only in the contact zone, but also in the inclined wall in the vicinity of the contact zone. Finally, the results also suggested that the fracture tends to appear at the transitional zone between the contact area and formed wall. However, the model presents a limitation in that the plane strain assumption is valid only for axisymmetric components.

In contrast, Jackson and Allwood [63] experimentally examined the deformation mechanics of specially prepared copper sheets formed using SPIF and TPIF and found the mechanism to be stretching and shear in the plane perpendicular to the tool direction, with shear in the plane parallel to the tool direction. While that was a pure experimental effort, Malhotra et al. [6] used a damage plasticity model together with FE analyses and experimental comparisons to report that fracture in SPIF was controlled by both local bending and shear. Local stretching and bending of sheet on the tool vicinity originated from higher plastic strain on the outside surface of the sheet increasing damage as compared to the inner surface. The shear effect in SPIF delayed damage accumulation while high local bending of the sheet around the tool caused greater damage accumulation in SPIF than in conventional forming. Although these opposing phenomena result in higher damage accumulation overall in SPIF, formability is still higher in SPIF. This has been explained using a ‘noodle theory’ which suggests that as the deformation in SPIF is inherently local, a large region of unstable but non-fractured material is generated before actual failure occurs. This region shares the deformation in subsequent tool passes. One of the limitations of this work, however, is that kinematic hardening and sheet anisotropy are not considered in the developed fracture model. Furthermore, the effects of variations in strain rate for strain rate sensitive materials were not considered.

It was claimed that both through-the-thickness shear and local bending of the sheet around the tool were influential in deciding the onset of fracture. The effect of through thickness shear (TTS) has been analysed in detailed by Eyckens et al. [64-66]. This work extended the Marciniak–Kuczynski (MK) forming limit model in order to predict the localised necking in sheet metal forming operations in which TTS occurs [67-69]. The FLD of a purely plastic, isotropic hardening material with von Mises yield locus was discussed, for monotonic deformation paths that include TTS. Formability increases based on TTS was explained through a detailed study of some selected deformation modes. The case study showed that the presence of TTS in the plane is related to the critical groove direction in MK model. TTS allowed a change of strain mode resulting in a delayed of necking. Formability predictions were seen to be greatly affected by the direction of applied TTS in the major in-plane strain direction. This last result was in contrast to the results obtained with the model of Allwood et al. [70] which predicts no effect of the direction of TTS on formability.

In more recent work, Gatea et al. [71] developed a modified Gurson–Tvergaard–Needleman (GTN) model that can be used to predict ductile fracture in SPIF. In this study, parameters for the model were determined using tensile tests, which included the void volume fraction. Under external loading leading to plastic strain, void formation around non-metallic inclusions and second phase particles started a nucleation mechanism. The voids increase in size going beyond a critical value ultimately tearing the ligaments between enlarged voids causing fracture perpendicular to the tensile loading direction. For the grade-1 Ti specimen used, the void volume fraction at fracture was recorded as 0.3025 compared to 0.00138 prior to deformation. The predicted fracture depth in ABAQUS using this model for hyperbolic cone was 31.68 mm as opposed to 30.29 mm as observed in experiment, which gives a less than 5% error margin.

3.2 Forces in SPIF.

One of the key considerations in the design or selection of an incremental forming setup is the forming force. In general, milling machines are not designed to bear high forces perpendicular to the spindle axis [29], and most CNC machines do not have an in-built apparatus for force measurement limiting the possibility of monitoring forces in-process without building a custom rig for the same. This calls for force estimation modeling, and extensive work on the same using analytical, semi-analytical, empirical and numerical approaches has been carried out.

Of the different models, the one provided by Aerens et al. [51, 69, 72, 73] has been widely used. It provides a force prediction model based on experiments done on several materials and variation of experimental parameters such as sheet thickness and tool diameter. This model relates the tensile strength of the material to the force in the axial direction by the following relation:

$$F_z = 0.0716 R_m t^{1.57} d_t^{0.41} \Delta h^{0.09} \alpha \cos \alpha \quad (1)$$

where, R_m is the ultimate tensile strength expressed in N/mm², t is the sheet thickness expressed in mm, d_t is the tool diameter in mm, Δh is the scallop distance measured in mm and α is the wall angle in degrees. Fig. 4 shows the typical force variation that is expected during a SPIF operation. This model has been

validated by benchmarking experiments done by several researchers [74, 75], and also by comparison with finite element simulations as in Eyckens et al. [69].

It may however, be noted, that the Aerens model does not account for strain hardening and sheet anisotropy, while bending is only indirectly considered. While strain hardening increases the strength of the material, thereby increasing the resulting contact force between the tool and sheet, anisotropy in the rolling and transverse directions implies that the ultimate tensile strength is different in the two directions and hence, the force measurement will be affected by the same depending on the region that the tool is processing. One of the advantages of this analytical model, however, is that it is much faster to come up with an estimate of the steady state force using the analytical model enabling quick selection of process parameters for forming, while finite element models that take into account anisotropy and strain hardening take a long time to calculate. In more recent work, Li et al. [76] have proposed a force model for the tangential force considering the deformation modes of stretching, bending and shearing. However, as this is much recent work, validation by other researchers is not yet available for this modelling.

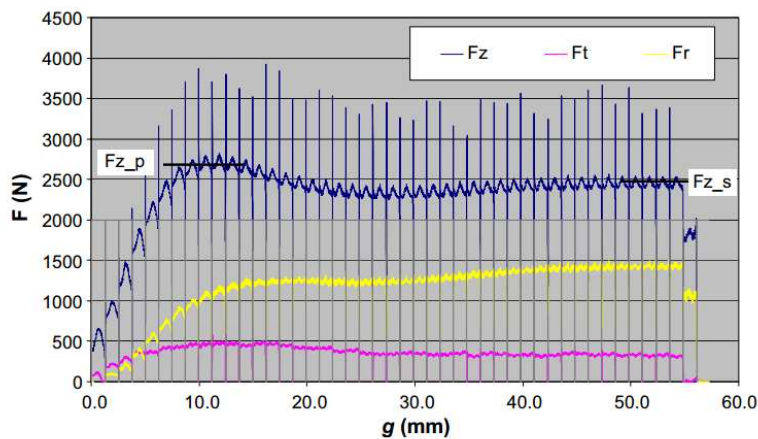


Fig.4. Force variation for a DC01 steel sheet of thickness 1.15 mm with wall angle 60°, tool diameter 25 mm, depth increment 1.06 mm plotted against ‘g’, the length of the generating line of the cone; Fz is the axial force, Fr the radial force and Ft the tangential force [51] [with permission from publisher]

3.3 Toolpath strategies

Several efforts have been made to investigate the effects of different types of toolpath strategies on the final formed part. The use of a z-level contouring toolpath with incremental step down depths results in a final part with these indentations clearly visible, typically as a line or curve along which the tool has stepped down. Furthermore, the axial force peaks at every step down. To overcome this, a helical toolpath may be used, as proposed by Skjødt et al. [77] Fig. 5 shows the difference between the two toolpath strategies. The helical toolpath not only eliminates the scarring caused by contouring toolpaths but also eliminates the axial force peaks.

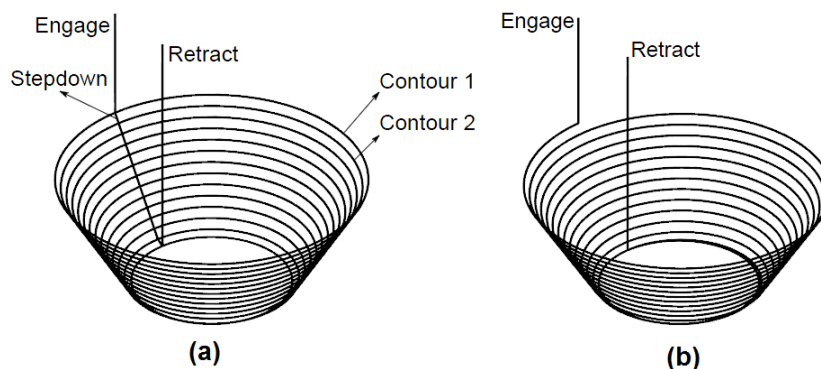


Fig.5. Toolpath strategies for SPIF showing (a) z-level contouring toolpath (b) helical toolpath [43] [with permission from publisher]

In addition, toolpath strategies have been designed to overcome the three major issues in SPIF, viz.: i) process limits, ii) accuracy and iii) thickness variations. While Table 2 summarizes these efforts, details can be found in the next three sections covering both hardware and toolpath based approaches to overcome the limitations of SPIF.

Table 2. Summary of work on toolpath strategies

Method(s)	Authors	References
Simple compensation using mirroring, pre-forming	Bambach et al.	[78]
Kinematic tool, backing plate effect and bottom forming	Essa et al.	[15]
Feature based correction (FSPIF), Robot assisted SPIF, Laser-assisted SPIF, Multi-step	Verbert et al.	[43], [5, 32, 40, 79]
Online toolpath correction	Rauch et al.	[80]
Multi-step technique, helical toolpaths	Skjødt et al.	[77, 81]
Back-drawing incremental forming, analytical correction, deep geometries correction	Filice et al.	[82-87]
Hardware and online feedback system	Allwood et al.	[29]
Graph topological approach, intelligent sequencing, multi-step mesh morphing	Behera et al.	[10-12, 14, 88-91]
Feature based techniques	Lu et al.	[20]
Mixed toolpaths, spiral toolpaths	Cao et al.	[92, 93]

3.4. Thickness variations

Incremental forming is characterized by a reduction in the wall thickness of the final manufactured part compared to the original sheet thickness. The final thickness t_f for single pass uncompensated toolpaths is an approximate function of the initial thickness t_0 given by the relation:

$$t_f = t_0 \cos(\alpha) \quad (2)$$

where, α is the wall angle

Thickness control can be achieved by using multi-pass toolpaths as shown by Duflou et al [5]. Azaouzi et al.[94] developed a method for optimizing the toolpath for a test case using a combination of response surface methods used with sequential quadratic programming creating a homogenous distribution of thickness for a specific test case. In other studies, Duflou et al. [95] found that for a pyramidal part, one could observe a distribution of thickness with increase in thickness on a planar face in the direction of tool movement up until the location of semi-vertical ribs for 1.5 mm thick AA 3103 parts with high wall angles close to failure. This distribution of thickness, as shown in Fig. 6 was found to be correlated to the so-called “inverse twist effect”, where grid movement is observed in pyramidal parts in a direction opposite to the tool movement direction [95, 96].

New optimization techniques for thickness control are also being designed for better thickness control in incremental forming. For instance, Malhotra et al. proposed the accumulative double sided incremental forming technique which results in a more uniform thickness profile compared to SPIF [97].

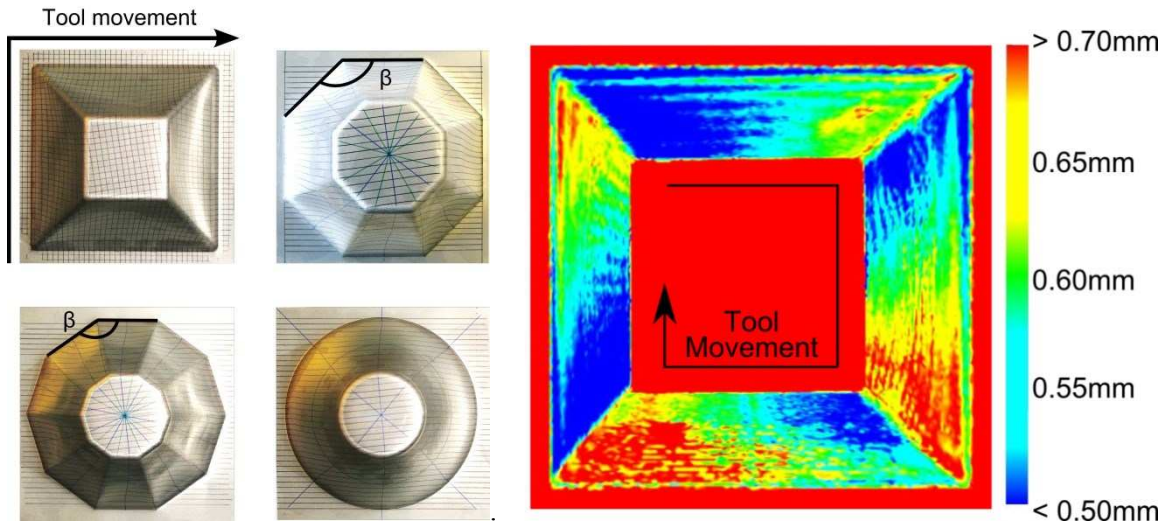


Fig.6. Twist effect in unidirectional contouring toolpaths for different shapes (left) and thickness plot for a pyramid of wall angle 70 made of AA 3103 (right) [95] [with permission from publisher]

Mirnia et al. [98, 99] have used sequential limit analysis to predict and optimize thickness distribution in incremental forming. They claim that this technique has proven to predict thickness faster than conventional finite element analysis. The effects of various deformation paths on final thickness distribution were studied and thickness distribution could be improved for a cone with wall angle of 70° by using intermediate shapes that have different radii than the final shape.

3.5 Technology assessment and future guidelines

The process fundamentals of SPIF are now understood in significant detail and the developed models for formability and force predictions have been tested and verified independently by different research groups. While forming limits for SPIF tend to be higher than conventional processes, these are still quite low for a number of materials, thereby delaying commercial exploitation. The incorporation of these forming limits within software codes for SPIF can be used for generating intelligent tool paths that are optimized for thickness and accuracy variations. However, as the available forming limits are obtained with differing process parameters, a unified database for SPIF is currently lacking and requires close collaboration among research groups to exchange accumulated process data over the last decade. This is essential for developing the next generation of process planners for SPIF. Furthermore, in-process online force measurements can alleviate the need for accurate force models, and such measurements can potentially be used for controlling dimensional accuracy in the future.

It is noticeable that research on sheet thickness variations has been limited. This is particularly because of the dependence of sheet thickness primarily on geometry. However, multi-step strategies can result in thickness profiles that cannot be easily calculated and may need simulations. Control of thickness variations could affect other process outcomes such as dimensional accuracy as both are dependent on the tool paths used, and hence, simultaneous control is an area that can be researched in the future.

4. Process Window Enhancement

Since incremental forming is limited by process limits leading to failure in parts with high wall angles, strategies need to be developed that can extend these limits. The different approaches to enhance process limits can be categorized into i) multi-step toolpath strategies, ii) workpiece orientation and iii) thermal methods that heat up the sheet in-process using lasers, electricity, etc.

4.1 Multi-step SPIF.

Duflou et al. [5] and Skjødt et al. [81] proposed multi-step toolpaths that allowed the manufacture of parts with wall angles of 90° and more. Fig. 7 (a) and (b) show the contours and strain distribution in the multi-

step manufacture of a cone, and a pressure vessel mold with cylindrical wall. Efforts have been made to optimize the multi-step process. Liu et al. [100] analyzed three different techniques of carrying out multi-step SPIF, viz.: i) increasing diameter of part in step ii) increasing wall angle in steps and iii) increasing part height and wall angle in steps. A combination of increasing diameter and wall angle in steps was found to be the most effective strategy. Prediction of thickness in multi-step SPIF can now be done using a geometric calculation of intermediate shapes and tracing back nodal points of the punch [101]. However, multi-step SPIF can result in a stepped feature at the bottom of the part. This can be attributed to rigid body motion and can be smoothed out by using a combination of in-to-out and out-to-in toolpaths [102, 103]. In-to-out toolpaths are generated by considering toolpaths from the center of the blank towards the peripheral edge, while out-to-in are generated in the opposite direction, as shown in Fig. 7 (c) and (d). Analytical equations were developed to predict the rigid body motions. These equations have constants which depend on the mechanical behavior of the sheet material and sheet thickness, but are independent of the intermediate shapes formed in multi-step SPIF. Numerical simulations can be used to find these constants. This approach was shown to be successful for axisymmetric components only in this work, including the forming of a cylinder with wall angle of 90° .

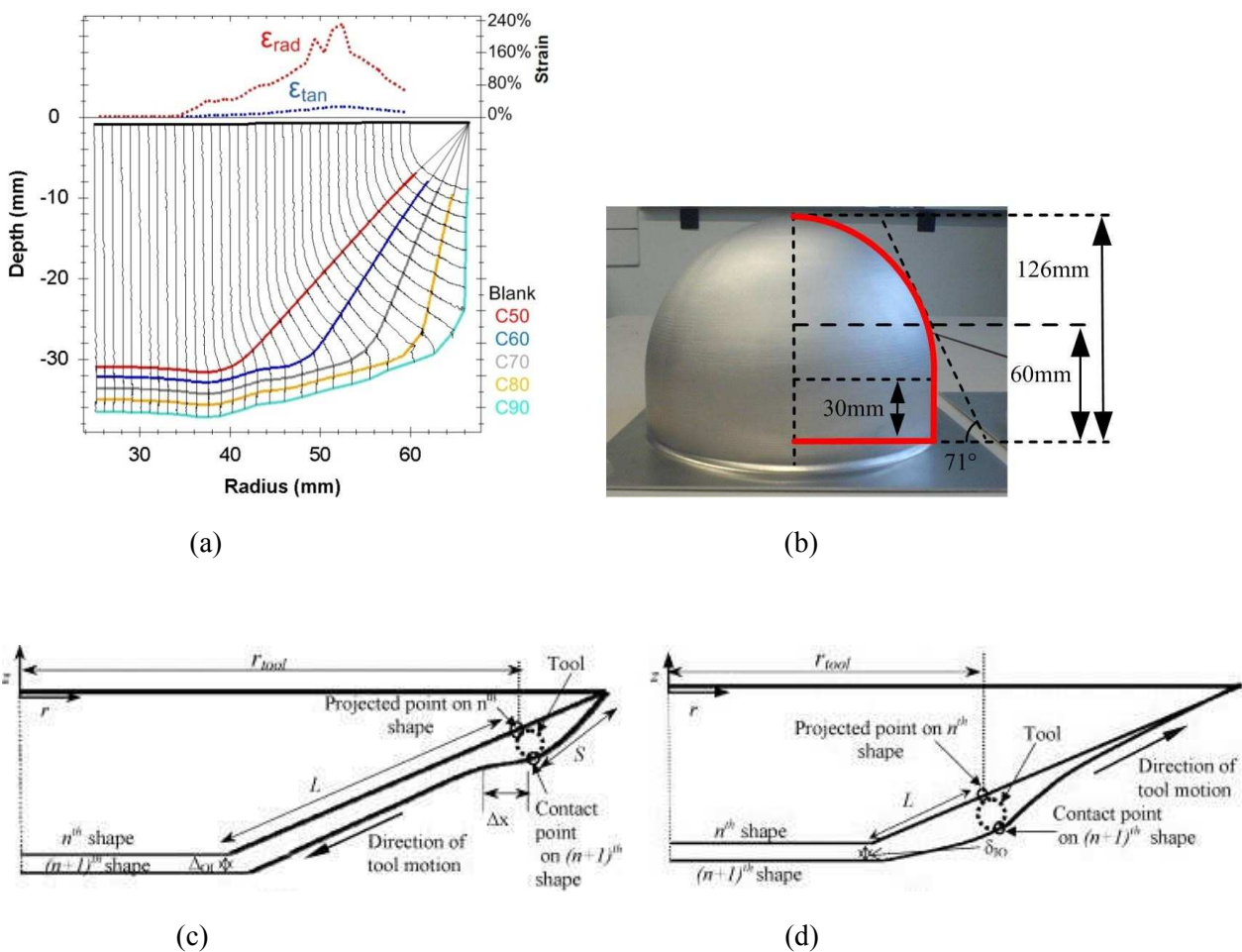


Fig.7. (a) Contours and strain distribution for a cone of 90 degrees made with multi-step toolpaths in five steps (b) a pressure vessel mold with cylindrical walls manufactured with this technique (right) [5, 43] (c) out-to-in toolpath (d) in-to-out toolpath [102, 103] [with permission from publisher]

4.2 Optimized workpiece orientation.

Another technique of increasing the process limits is by optimal orientation of the workpiece, and creating angled toolpaths, as illustrated by Vanhove et al. [104]. This allows local forming of a region with a wall angle higher than the failure wall angle by rotating the plane of the workpiece in an optimised way. Without changing the geometry of the work piece, this strategy virtually lowers the wall angle in the targeted region while increasing the wall angle in other regions, as shown in Fig. 8.

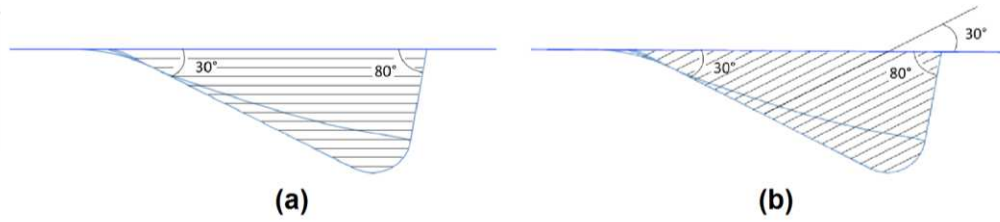


Fig.8. Conventional toolpath shown in (a) compared with angled toolpath shown in (b) [104] [with permission from publisher]

4.3 Heat Supported SPIF.

While approaches to modifying toolpaths and workpiece orientations do increase formability, it may not be feasible to do so for parts with complex shapes, and hence, approaches that take advantage of the material behavior have also been proposed. A number of techniques have been developed, as summarized by Xu et al. [105]. These include heating using conduction, convection, radiation, friction, electricity and hybrid techniques such as employing a combination of electric and friction heating. Table 3 summarizes the specific efforts that have been made together with the formed material.

Hot SPIF using a heater band for magnesium alloy, AZ31, revealed a maximum formability temperature of 250° C [106]. A patented process by Duflou et al. uses the technique of dynamic local heating where a laser source is used to heat up the workpiece surface at a small spot that follows the position of the deforming tool with a small offset [40]. Using this technique, the formability of 0.5 mm 65Cr2 sheets was increased from 57° to 64°, and for 0.6 mm TiAl6V4 sheets the critical wall angle for failure improved from 32° to 56° [40]. Fig. 9 shows a schematic of this setup. Göttmann et al. [107] have demonstrated the use of the same principle, but by using the laser on the same side as the forming tool and applied it to both SPIF and TPIF. While improvement in formability was observed for TiAl6V4, there was no improvement for Ti grade 2 in this work.

Another thermal method that has been used is electric hot forming which has been attempted by Fan et al. [108, 109] and Ambrogio et al. [110]. Fan et al. [109] investigated the effect of current, tool size, feed rate and step size on the formability of AZ31 magnesium achieving a maximum failure wall angle of 64.3° at a current of 500 A. They also found that asymmetric parts (such as pyramids) show more distortion than axisymmetric parts (such as cones). In other work, Palumbo et al. [111] have demonstrated that tool rotation creating friction in SPIF can act as a stabilizing necking phenomena thereby enhancing formability.

Of the different hot SPIF approaches, Xu et al. [112] report that friction-stir and electric hot SPIF offer the best choices. They compared these two techniques and found that in the processing of magnesium alloy AZ31B sheets of 1.4 mm thickness, friction-stir was more efficient in forming truncated funnel shapes while electric hot SPIF led to faster heating thereby limiting the effect of component geometry on formability.

Table 3. Summary of heating techniques used for SPIF

Heating principle	Sheet material	Authors	Reference
Convection	AZ31	Ji and Park	[113]
Conduction	AZ31	Ambrogio et al.	[106]
Radiation	65Cr2, TiAl6V4	Duflou et al.	[32]
Radiation	Ti grade 5	Göttmann et al.	[114]
Friction	A2017-T3	Otsu et al.	[115]
Friction	AA 5052-H32	Xu et al.	[116]
Electric	AZ31, TiAl2Mn1.5	Fan et al.	[109]
Electric	AA2024-T3, AZ31B-O, Ti6Al4V	Ambrogio et al.	[110]
Electric	AA 5055, AZ31	Sy and Nam	[117]
Electric+friction	TiAl6V4	Palumbo and Brandizzi	[111]

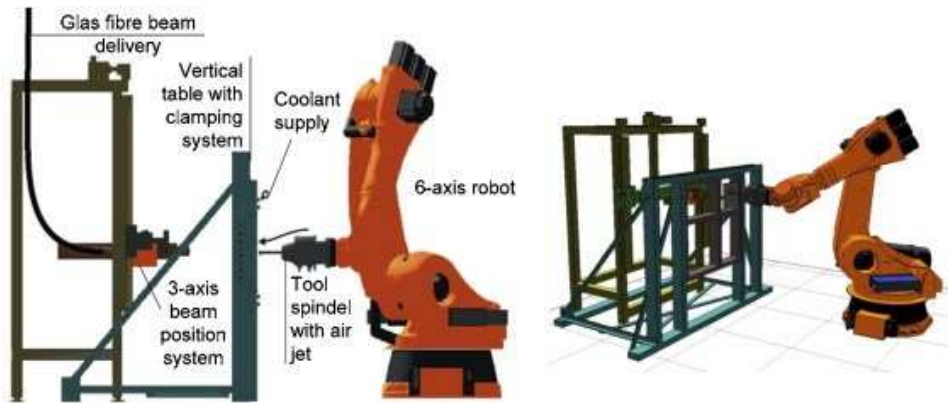


Fig.9. Patented laser assisted SPIF setup developed at KU Leuven [40] [with permission from publisher]

4.4 Other process variants.

A few other process variants have been developed to enhance process windows. An electromagnetic incremental forming process (EMIF) to enable forming of large parts has been developed [118]. Here, the solid conventional punch is replaced by an electromagnetic coil with no mechanical contact whatsoever with the sheet being formed, as shown in Fig. 10. Energy stored in a capacitor bank is discharged through the coil creating a magnetic field, which induces an eddy current on the sheet blank. Repulsive forces between the coil and the sheet drive the sheet towards a mold over which the part gets formed in incremental steps. Improvements in surface roughness and forming time were observed. A cryogenic SPIF setup was also developed showing initial promise in extending process limits for specific aluminum alloys [60]. This used the principle that at cryogenic temperatures, there is enhanced tensile elongation for certain face centred cubic alloys, resulting in increased strain hardening. Vahdati et al. [119] have developed an ultrasonic vibration assisted setup. Tests were carried out on AA 1050-O sheets and their results showed improvement in forces, accuracy and surface finish of the formed parts. In experiments carried out with AA 1050-O sheets of 0.7 mm thickness, forming forces were found to reduce by 36 % while formability improved by 48 % when ultrasonic forming in the presence of a lubricant was performed [120].

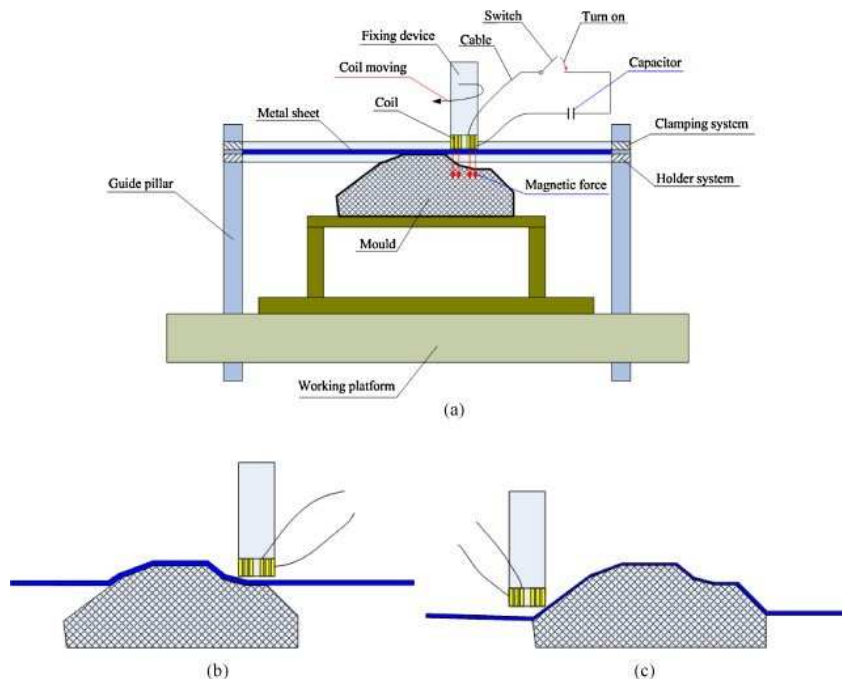


Fig.10. Schematic of EMIF setup [118] [with permission from publisher]

4.5 Technology assessment and future guidelines

Automating multi-step SPIF requires the development of systematic rules for incremental steps. In recent work, it has been shown that the final part shape can be systematically morphed into intermediate shapes that enables automated generation of multi-step toolpaths [121]. Using the mesh morphing strategy, a two slope pyramid with top plane wall angle of 80° and bottom plane wall angle of 25° was successfully formed with AA 3103 sheet of 1 mm thickness yielding a maximum deviation less than 1 mm compared to more than 10 mm without using the morphing technique. Exploration of optimized workpiece orientation in improving process limits has been minimal and can be combined in the future with multi-axes machine tool setups that enable the tool to process the workpiece in a manner so as to optimize the draw angles. While a number of efforts have focused on heat supported SPIF and different methods have been used to improve formability and accuracy, the results shown are for specific materials with experiments performed under varying operating conditions. Standardized guidelines for the use of these methods are unavailable and will require research groups to come together to set benchmarks in the future that enable process selection and intelligently setting the right operating parameters for forming specific parts. Without such a collective effort, experiments can go on forever given the wide range of alloys and combinations of process variables such as sheet thickness, punch diameter, spindle speed, feed rate, step down etc. The current literature also excludes looking into control of the heat source to improve process outcomes, which is important from an industrial applications perspective. Additionally, efforts to improve dimensional accuracy need to consider combining optimized tool path generation that compensates for spring back together with heat support.

5. Accuracy characterization and improvement

5.1 Accuracy issues and characterization

One of the key issues in incremental forming is that of the achievable accuracy. Jeswiet et al. [3] report that, while most industrial parts require an accuracy of ± 0.5 mm, it is observed that parts produced by SPIF have significantly higher dimensional inaccuracies. The absence of a supporting die on the free surface of the sheet blank does not allow geometric accuracy achieved to be beyond a certain limit. The accuracy realized in incremental forming is also dependent on the stiffness of the setup used [43]. In general, milling machines are stiffer than industrial robots, and hence, parts made on milling machines tend to be more accurate. Fig. 11 shows a comparison of the accuracies realized on an Aciera 3-axis milling machine vis-à-vis a KUKA industrial robot.

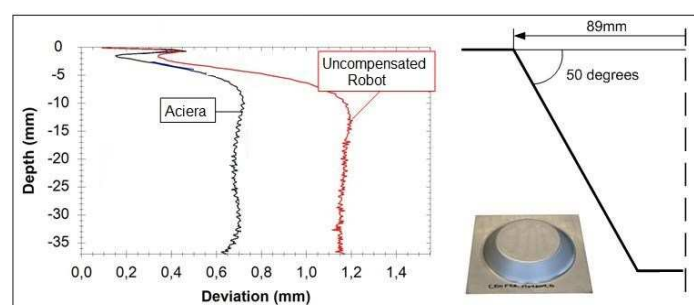


Fig.11. Accuracy comparison between an Aciera milling machine and an uncompensated robot for a cone of wall angle 50° [43] [with permission from publisher]

The accuracy of a part is also dependent on the geometrical features present in the part. Verbert [43] classified features into four categories based on their behavior, viz.: planes, ruled, freeform and ribs and developed the Feature-assisted Single Point Incremental Forming (FSPIF) technique to detect features in a part. The accuracy of these features is also dependent on the wall angles within the feature. In general, for most materials and sheet thicknesses, planar and positive curvature features with low wall angles tend to over form, while high wall angles tend to under form.

Several studies in incremental forming have involved the use of finite element analysis to predict the final shape and dimensional deviations [8, 122-124]. Hadoush et al. [123] have mentioned computation times for

such analyses to vary from 16 hours to a few days for a simple pyramidal part of depth 20 mm with 40 incremental steps of 0.5 mm each, using implicit iterative algorithms. The computation time for convergence is also dependent on the geometry and size of the part, and is a major limitation to the application of finite elements as a quick accuracy prediction tool. Guzmán et al. [125] found by means of their simulation studies that the dimensional inaccuracies in a two-slope pyramid formed by SPIF can be attributed to elastic strains caused by structural elastic bending in addition to local spring back.

5.2 Accuracy improvement strategies

Several strategies to improve accuracy in incremental forming have been summarized by Micari et al. [82] and Essa et al. [15], including the use of flexible support, use of counter pressure, multipoint and backdrawing incremental forming and use of optimized trajectories. For robot supported incremental forming, Verbert et al. [27] took into account robot kinematics, and computed the deflection of the tool using the compliance of each joint defined as an angular deflection as a function of the moment load applied to each joint. Bambach et al. [78] proposed a combination of multi-stage forming and stress-relief annealing to improve the accuracy of a car fender section. The accuracy of parts with areas containing positive curvature or planar faces can be improved by reprocessing the workpiece [126] or using a reverse finishing operation [79]. However, this leads to a significant increase in the production time, and also yields a poor surface finish. Another method that has been proposed involves using measurements of the part to iteratively correct the CAD model by translating it by a scaled measure of the deviations for each individual point [127]. The drawback of using such a strategy lies in its lack of suitability for parts that need to be manufactured only once or in small batches, and the application of such a strategy would require making test parts, measuring them and then applying the correction strategy, possibly in an iterative procedure. Rauch et al. [80] propose an online toolpath optimization technique that is aimed at improving accuracy and surface roughness, as shown in Fig.12. However, this study is limited to the depth accuracy and the accuracy of the complete part is not addressed using this technique.

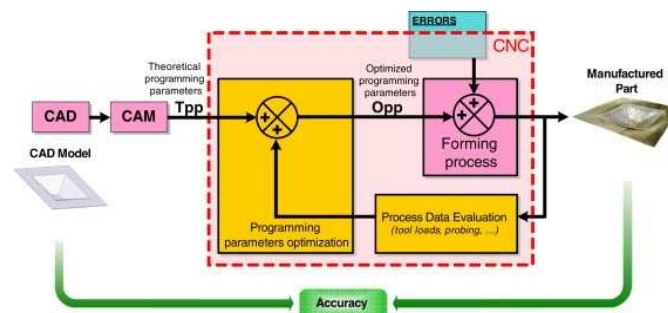


Fig.12. Intelligent CAM programming approach to optimizing toolpaths [80] [with permission from publisher]

An automated spiral toolpath generation technique has been developed which takes geometric accuracy, forming time and scallop height as input constraints [93]. A mixed toolpath strategy with a combination of in-to-out and out-to-in toolpaths that helps create a smooth component base in multi-step SPIF has also been tested [103]. A model-based path planning system has been developed that takes into account machine element compliances for a two robot assisted incremental forming setup and spring back deviation predictions [128]. Earlier, Duflou et al. [40] have demonstrated the improvement of accuracy in laser-assisted SPIF using uncompensated toolpaths while Mohammadi et al. [129] have proposed in-process laser-assisted hardening to create regions in a sheet metal part with high stiffness thereby reducing the effect of interactions between different features and improving the accuracy of the final part. Besides, Micari et al. [83] have tried to model the errors at the bottom corner and under forming of the bottom using geometrical parameters such as sheet thickness, part geometry and process variables such as tool diameter and step down. In other attempts, Fiorentino et al. [130] have used an artificial cognitive system based on iterative learning control to improve part precision. In addition to these isolated efforts, one of the significant achievements in the last 10 years has been systematic compensation using error correction functions that use accuracy response surfaces and graph topological tool path planning discussed next.

The compensation of part geometry to account for inaccuracies can be realized by predicting the formed shape. Behera et al. [12] have used Multivariate Adaptive Regression Splines (MARS) to predict the

behavior of planar features, ruled features, and interactions between these features for AA 3103 of 1.5 mm. Later, this work was extended to include other materials such as DC01 and AA 5754 [88] and eventually generic error correction functions were developed [60]. In later work, this method was extended to freeform features approximated as ellipsoids, leading to the accurate manufacture of cranial implants [14]. Table 4 summarizes the response surface models from these efforts. The presence of a multitude of features on complex parts leads to multiple inaccuracy inducing phenomena occurring simultaneously due to interactions between the features. To overcome this, a network analysis methodology has been proposed using topological conceptual graphs to capture the effects of different phenomena on the final accuracy of a sheet metal part manufactured by SPIF [10]. Toolpath generation algorithms to create partial toolpaths that account for the accuracy of specific features in the part based on the proposed framework were discussed here. Finally, the creation of integrated toolpaths maintaining complementarity between toolpaths and desired continuity behavior using non uniform cubic B-splines was illustrated. The manufacture of a human face part with significantly high accuracy using this methodology was illustrated as shown in Fig. 13.

In recent work, attempts have been made to use data mining techniques using a local geometry matrix representation that creates a classifier [131] and point series based surface representation techniques [132] to predict spring back. Although formed surfaces have been predicted using these techniques, the errors are of the order of 1 mm, and the loop has not been closed with respect to actually manufacturing accurate parts by using these predicted surfaces to compensate geometries. Another issue of importance is that of part trimming as parts need to be trimmed often at the top contour for real applications. Trimming can induce significant distortion in the final part due to compressive stresses generated during SPIF. This can be alleviated by using stress relieving heat treatment as applicable to the sheet material that was formed [133].

5.3 Technology assessment and future guidelines

Due to significant work done in the past decade on accuracy, complex parts can now be formed with dimensions consistently less than 1 mm maximum deviations. However, the accuracies realized are valid only for parts with dimensions typically less than 200 mm x 200 mm x 100 mm. For large sized parts, only a limited number of scaling studies have been performed. The use of regression based compensation for large sized parts is bound to be limited as that would require generating training sets with large parts, which in turn call for long forming times, use of large quantities of sheet blanks and time required for metrology using laser scanners or touch probes. Hence, new tooling based approaches to improve dimensional accuracies must be forthcoming. Furthermore, the accuracies realized using emergent heat supported SPIF techniques have not been systematically characterized yet. The combination of tool path compensation and strategies to enhance process limits have only been explored to a limited extend and require further investigation. Although tool path compensation software is now available, this needs to be integrated with traditional CAD packages to enhance usability. Furthermore, given the wealth of data among the different research groups involved in SPIF, accuracy data can potentially be collated to carry out data mining and improving existing models for predicting accuracy behavior.

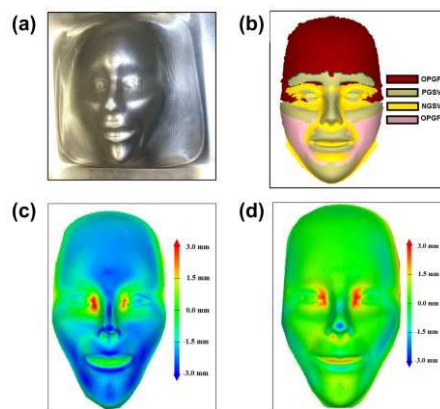
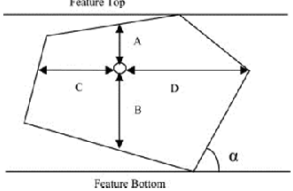
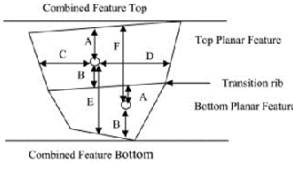
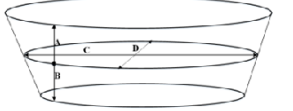
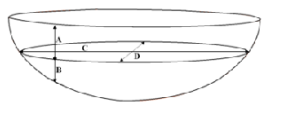


Fig.13. 3D Human Face Mask Manufacture using graph topological analysis [10] [with permission from publisher]

Table 4. Accuracy response surface models using Multivariate Adaptive Regression Splines (MARS) for various geometries

Model geometry	Representative diagram	Material	Thickness	Equation	Reference
Planar		AA 3103	1.5 mm	$e = 2.4 - 0.76 * \max(0, d_b - 0.4) - 1.2 * \max(0, 0.4 - d_b) - 2.3 * \max(0, d_b - 0.78) + 2.8 * \max(0, d_b - 0.44) - 3.4 * \max(0, 0.44 - d_c) - 3.3 * \max(0, d_o - 0.65) - 0.058 * \max(0, d_h - 113) - 0.0082 * \max(0, d_h - 127) + 0.034 * \max(0, d_h - 143) + 0.055 * \max(0, d_v - 71) + 0.010 * \max(0, 71 - d_v) - 3.5 * \max(0, 1.1 - \alpha)$	[12]
Ruled	Same as planar without C and D	AA 3103	1.5 mm	$e = 1.2 - 1.9 * \max(0, d_o - 0.13) + 1.5 * \max(0, d_o - 0.26) + 0.0024 * \max(0, d_v - 13) - 0.054 * \max(0, 13 - d_v) - 0.0021 * \max(0, d_v - 30) + 0.0042 * \max(0, d_v - 78) - 5.6 * \max(0, k_m - (-0.012)) - 6.9 * \max(0, -0.012 - k_m) - 0.4 * \max(0, \alpha - 2.3) + 0.72 * \max(0, \alpha - 2.4) - 1.1 * \max(0, 2.4 - \alpha) - 1.6 * \max(0, \alpha - 2.4) + 3.1 * \max(0, \alpha - 2.5)$	[12]
Planar-Planar interaction		AA 3103	1.5 mm	$e = 1.2 - 0.018 * \max(0, d_b - 109) - 0.0028 * \max(0, 109 - d_b) + 3.1 * \max(0, \Delta\alpha - 0.35) + 0.15 * \max(0, 0.35 - \Delta\alpha) + 4.5 * \max(0, d_f - 0.28) - 7.8 * \max(0, d_f - 0.57) - 2.1 * \max(0, 0.57 - d_f) - 30 * \max(0, d_f - 0.93) + 0.018 * \max(0, d_e - 46) - 0.0068 * \max(0, 46 - d_e) - 2.6 * \max(0, d_e - 0.18) + 4 * \max(0, 0.18 - d_e) + 2.4 * \max(0, d_e - 0.51) + 7.3 * \max(0, d_e - 0.89) - 5.6 * \max(0, 0.87 - \alpha)$	[12]
Ruled-Ruled interaction	Same as planar-planar interaction without C and D	AA 3103	1.5 mm	$e = 1.3 - 13 * \max(0, d_f - 0.94) + 0.4 * \max(0, 0.94 - d_f) - 0.04 * \max(0, d_e - 81) + 0.027 * \max(0, d_e - 134) - 0.041 * \max(0, 134 - d_e) + 7.8 * \max(0, \alpha - 2.2) - 18 * \max(0, \alpha - 2.6) - 12 * \max(0, \alpha - 2.7) + 3.4 * \max(0, 2.7 - \alpha) - 36 * \max(0, \Delta\alpha - 0.44) + 32 * \max(0, \Delta\alpha - 0.52) - 2.6 * \max(0, 0.52 - \Delta\alpha) + 4.1 * \max(0, \omega - 0.98) - 16 * \max(0, \omega - 1.1) + 3.3 * \max(0, 1.1 - \omega)$	[12]
Planar-Planar interaction	Same as Planar-Planar interaction for AA 3103	AISI 304	0.4 mm	$e = 0.84 + 0.27 * \max(0, d_b - 0.48) + 1.4 * \max(0, 0.48 - d_b) + 1.1 * \max(0, d_o - 0.32) + 4.3 * \max(0, 0.32 - d_o) - 0.017 * \max(0, d_h - 101) - 0.011 * \max(0, 101 - d_h) + 0.2 * \max(0, d_h - 150) + 0.11 * \max(0, d_v - 54) - 0.35 * \max(0, d_v - 62) + 0.023 * \max(0, 62 - d_v) + 5.2 * \max(0, \Delta\alpha - 0.26) - 3.4 * \max(0, 0.26 - \Delta\alpha) - 6.4 * \max(0, d_f - 0.54) - 3.8 * \max(0, 0.54 - d_f) - 0.016 * \max(0, 108 - d_e) + 2.1 * \max(0, \alpha - 0.52) + 1.9 * \max(0, 0.52 - \alpha)$	[88]
Planar-Planar interaction	Same as Planar-Planar interaction for AA 3103	AlMg3	1 mm	$e = 2.6 + 0.97 * \max(0, d_o - 0.39) + 4.1 * \max(0, 0.39 - d_o) + 25 * \max(0, d_o - 0.9) - 0.031 * \max(0, d_h - 117) - 0.0053 * \max(0, 117 - d_h) - 0.33 * \max(0, d_v - 62) + 0.043 * \max(0, 62 - d_v) + 2.5 * \max(0, \Delta\alpha - 0.35) - 3.3 * \max(0, 0.35 - \Delta\alpha) - 5.1 * \max(0, d_f - 0.58) - 5.3 * \max(0, 0.58 - d_f) - 52 * \max(0, d_f - 0.92) - 0.039 * \max(0, d_f - 63) + 0.056 * \max(0, d_e - 82) - 0.058 * \max(0, 82 - d_e) + 21 * \max(0, \alpha - 0.96) - 2.6 * \max(0, 0.96 - \alpha)$	[88]
Planar-Planar interaction	Same as Planar-Planar interaction for AA 3103	DC01	1 mm	$e = 2.2 + 0.37 * \max(0, d_o - 0.44) + 2.6 * \max(0, 0.44 - d_o) + 23 * \max(0, d_o - 0.9) - 0.027 * \max(0, d_h - 117) - 0.057 * \max(0, 117 - d_h) - 0.22 * \max(0, d_v - 62) + 0.032 * \max(0, 62 - d_v) + 2.9 * \max(0, \Delta\alpha - 0.17) + 0.75 * \max(0, 0.17 - \Delta\alpha) - 4.2 * \max(0, d_f - 0.6) - 4.4 * \max(0, 0.6 - d_f) - 45 * \max(0, d_f - 0.92) - 0.032 * \max(0, d_e - 63) + 0.047 * \max(0, d_e - 82) - 0.049 * \max(0, 82 - d_e) + 16 * \max(0, \alpha - 0.96) - 2.5 * \max(0, 0.96 - \alpha)$	[88]
Ruled		Ti grade 1	0.5 mm	$e^r = 0.3 - 0.28 * \max(0, 0.96 - d_o) - 21 * \max(0, d_o - 0.96) - 0.096 * \max(0, 11 - d_v) - 0.0022 * \max(0, d_v - 11) - 0.006 * \max(0, 108 - l^{max}) + 0.46 * \max(0, l^{max} - 108) + 0.049 * \max(0, 31 - l^{min}) - 0.0035 * \max(0, l^{min} - 31) + 5.3 * \max(0, l^{min} - 94) - 8.5 * \max(0, 0.13 - k^{max}) - 27 * \max(0, k^{max} - 0.13) + 3.1 * \max(0, 0.25 - \alpha) + 19 * \max(0, \alpha - 0.25) - 18 * \max(0, \alpha - 0.36) - 0.32 * \max(0, 1.4 - \omega) - 0.34 * \max(0, \omega - 1.4)$	[14]
Freeform		Ti grade 1	0.5 mm	$e = -0.65 + 0.35 * \max(0, 0.97 - d_o) + 7.2 * \max(0, d_o - 0.97) - 0.024 * \max(0, d_v - 45) + 0.0049 * \max(0, 56 - d_v) + 0.71 * \max(0, d_v - 56) - 0.008 * \max(0, l^{max} - 97) + 0.028 * \max(0, 17 - l^{min}) + 0.013 * \max(0, l^{min} - 17) + 3.9 * \max(0, k^{max} + 0.0061) + 14 * \max(0, 6.8 * 10^{-5} - k^{min}) + 6.3 * \max(0, k^{min} - 6.8 * 10^{-5}) - 1.4 * \max(0, 0.62 - \alpha) - 1.2 * \max(0, \alpha - 0.62) + 3.5 * \max(0, \omega - 1.2) + 0.59 * \max(0, 1.3 - \omega) - 13 * \max(0, \omega - 1.3)$	[14]

Nomenclature for models in Table 4

d_b : normalized distance from the point to the edge of feature in the tool movement direction
 d_o : normalized distance from the point to the bottom of the feature
 d_v : total vertical length of the feature at the vertex
 d_h : total horizontal length of the feature at the vertex
 α : wall angle at the vertex (in radians)
 ω : angle of the tool movement with respect to the rolling direction of the sheet (in radians)
 k_m : maximum principal curvature at the vertex
 d_f : normalized vertical combined feature distance below the vertex
 d_t : total vertical combined feature length at the vertex,
 d_e : normalized distance to transition horizontal rib
 $\Delta\alpha$: wall angle difference between top and bottom planar feature
 l^{max} : major axis length on slicing the feature at the depth of the point
 l^{min} : minor axis length on slicing the feature at the depth of the point
 k^{max} : maximum curvature at the point
 k^{min} : minimum curvature at the point

6. Process modeling and simulation

Numerical simulation of the SPIF process can be very demanding computationally primarily due to high nonlinearities given the small contact area constantly changing between the tool and the sheet surface, as well as the nonlinear material behaviour combined with non-monotonic strain paths [67]. An accurate estimation from the numerical simulation results, specially related to the prediction of the forces during the forming process, is important as it contributes to the safe use of the hardware. The prediction of forming forces is particularly important in the case of using adapted machinery not designed for the SPIF process. In the following, a review of numerical studies is presented in three sections: i) material models, ii) algorithms and methods and iii) domain decomposition methods.

6.1 Use of different constitutive material models

Different material models have been tested in the course of the last 10 years of simulation in SPIF. In early attempts, Bambach et al. [134] tested three different hardening laws in simulations of an axi-symmetric component formed by SPIF (i) von Mises plasticity with isotropic hardening, (ii) von Mises plasticity with combined isotropic and kinematic hardening and (iii) Hill'48 plasticity with isotropic hardening. The authors have used isotropic and mixed (isotropic/kinematic) hardening laws. Results obtained with the mixed hardening law presented a more accurate prediction than using a simple isotropic hardening law. However, the geometry of the part was better predicted when kinematic hardening was accounted for.

He et al. [135] studied several aspects associated with FEM simulation choices as well as material and process parameters of the SPIF process. This involved comparison between simulation results and experimental measurements for a conical part. Two FEM software packages, Lagamine built at the University of Liege and commercial FE software ABAQUS, were used in this study. The flow stress curve for the material AA 3003 was approximated by the Swift law, $\sigma = 180 (\varepsilon + 0.00109)^{0.21} (MPa)$. The Hill'48 yield criterion was employed to describe the plastic anisotropy during the deformation. For the cone shape, both codes gave almost identical results in the cone wall region, whereas the centre of the cone bottom obtained by Lagamine was about 2.3mm deeper than that from Abaqus. Different explanations were given to explain the differences in results, viz.: effect of different mesh densities, too stiff behaviour of the element used in Lagamine and too high penalty used in the Lagamine contact model.

Bouffioux et al. [136-138] developed an inverse method for adjusting the material parameters with experimental measurements. This involved doing line tests that deformed a flat blank along a pre-defined linear geometry and using the force data from these tests to tune the FE model. Strain evolution in SPIF has been studied using different finite elements to model the sheet and comparing with real time data obtained from digital image correlation (DIC) [54, 64]. Different plastic behaviours were considered, isotropic and

anisotropic yield criteria combined with either isotropic or kinematic hardening. The hardening law, Swift or Armstrong-Frederic, led to a low difference in strains. However, in all cases, the authors have mentioned this fact as being a forming process displacement-controlled, which means the strains are independent of the adopted material behaviour. In terms of forming force prediction, the dependence on the type of hardening law was more pronounced than the choice of yield criterion.

The influence of plastic behaviour on the accuracy of force prediction by FEM simulations has been studied [8]. These comparisons include the use of Swift and Voce hardening laws, isotropic or kinematic hardening models, isotropic von Mises and anisotropic Hill yield criteria. A less significant improvement in force prediction was obtained when taking into account kinematic hardening. Globally, the highest accuracy was reached using solid elements combined with a fine mesh, which used the isotropic yield locus of von Mises and the mixed isotropic–kinematic hardening model of Voce–Ziegler. The identification procedure based on the work of Bouffieux et al. [136] proved that the choice of the material parameters set cannot be made separately from the element type.

6.2 Simulation algorithms and methods

The simulation algorithms and methods require three important considerations, viz.: i) choice of integration schemes (explicit or implicit), ii) choosing the element type for simulation and iii) modeling the interaction between tool and sheet. These are discussed below.

6.2.1 Integration schemes: Explicit and Implicit

Both explicit and implicit time integration methods have been tried out by researchers in different simulation cases. Explicit integration within ABAQUS has been used for optimizing the toolpath [139]. The values of sheet thickness and geometry accuracy were compared with experimental results, along a radial section of a conical shape formed by SPIF. The results show no considerable influence of the friction coefficient on the prediction of geometry and thickness. Resorting to an implicit scheme combined with mass-scaling, the results did not considerably deteriorate. However, the calculation time increased from 30 minutes to more than three hours. A direct comparison of the predicted thickness using the explicit and implicit analyses demonstrated that the maximum difference between both schemes occurred at the vertical step down. This observation was due to the high kinetic energy transmitted through the tool during the sudden change from in-plane movement to the vertical increment. The obtained force also had a deviation when this vertical displacement was performed.

Yamashita et al. [140] used the dynamic explicit finite element code LS-DYNA to simulate the forming of a quadrangular pyramid with variations in its height. Several types of toolpaths were tested in order to find their effect on the deformation behaviour. The thickness strain distribution and the force acting during the tool travel were evaluated. According to the results, the density of the sheet material and the travelling speed of the tool cause inertial effect on deformation. They were pre-examined and optimised to determine the computational condition to use in the simulations in LS-DYNA, to reduce the computational time. The study concluded that numerical simulations using explicit schemes can be used for toolpath optimization in SPIF.

6.2.2 Finite element types

The performance of different element types available in ABAQUS has been tested [134]. These include 7 different types of solid elements and a shell element named S4R. The difference between the solid elements was the choice of anti-hourglass and anti-shear-locking modes. The finite element S4R is a shell element with reduced integration. For solid elements meshes, only two layers in the sheet thickness direction were used which is a minimum for modelling the bending state present in SPIF. The best results were obtained using the shell element, S4R. Numerical simulations using the reduced enhanced solid-shell (RESS) formulation have been performed comparing it with results from solid elements available in ABAQUS [141]. In this preliminary work, isotropic hardening and implicit analysis were considered. The RESS formulation showed equivalent accuracy to ABAQUS elements but using just a single layer of elements with user-defined integration points through thickness. Later on, the formulation was integrated in LAGAMINE code and coupled with a refinement-unrefinement mesh strategy resulting in significant reduction in CPU time [142].

6.2.3 Interaction between tool and sheet

Eyckens et al. [54, 69] used ABAQUS (standard implicit) for carrying out simulation of the process. In each model, the sheet was elasto-plastically deformed through contact with a hemispherical forming tool. The tool was modelled as a rigid surface and displaced and rotated with an angular velocity. The simulated contact pressure area between the tool and the sheet exhibited similar oscillations as the force components. It was found that at very low wall angles, such as 20° , the wall angle was responsible for the radial components of the forming forces to become nearly zero or even negative, which meant that the tool was pushed outwards instead of in the direction of the cone centre. A sub-modelling strategy improved the modelling of the plastic deformation zone in the SPIF simulation. However, the authors mentioned that the constitutive model of the sheet was too simple to accurately predict the forming force components while the quality of the forming force predictions was improved through the use of finer meshes.

Attempts were made to use FE simulations to explain the geometric deviations observed in SPIF taking into account the bending action of the tool [125]. In particular, it was important to find out if dimensional inaccuracies due to interactions between features could be well predicted by FE simulations and explain the causes behind the inaccuracies. Figure 14 shows the results obtained from this effort. It was reported that the main shape deviations come from elastic strains due to structural elastic bending and a minor contribution of localized springback. No plastic deformation was observed in the transition zone between two planar faces constituting the pyramid.

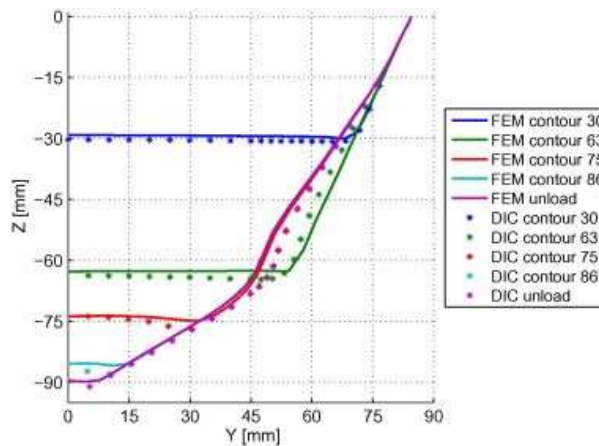


Fig.14. Comparisons between FE simulations and actual formed shape of a two slope pyramid [125] [with permission from publisher]

A simplified approach to simulate the contact between the tool and the sheet has been developed to reduce the CPU time of SPIF simulation [143]. In this model, the contact/friction with the rigid tools was replaced by imposed nodal displacements and a geometrical assumption for the successive local deformed shapes was employed. An algorithm was developed to find the nodes supposed to be in contact with the tool and to estimate their imposed displacements during a tool displacement increment. A parameter named “imposed displacement radius” (R_{imp}) was proposed to limit the contact area and it depends on distance L . The value of the distance L from the tool centre was based on several benchmark tests and was limited to 5 times the tool radius. R_{imp} can be determined as a function of the position of the tool centre, radius and a user parameter called Θ as shown in Figure 15.

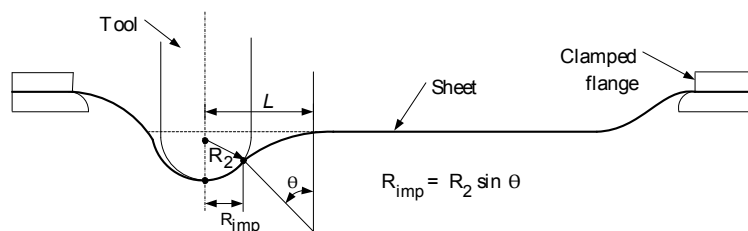


Fig.15. Geometrical assumptions for modelling the contact between tool and sheet [143] [with permission from publisher]

6.3 Domain decomposition methods

Domain decomposition methods include different approaches such as decoupling and sub-structuring. A decoupling algorithm has been used to reduce the computational time [144] where the decoupling algorithm consists of dividing the FE discretization into an elastic and an elastoplastic deformation zone. These two separated systems are solved in an alternating fashion resorting to an algorithm which results in a partial model providing boundary conditions for the other system. The boundary condition includes degrees of freedom and a number of elastic elements representing the elastic reaction of the remaining structure. The implementation of this decoupling method for enhancing the calculation performance reduced the system size. However, all approximations were still subject to a severe amplification of initial errors once the entire elastoplastic region was decoupled.

A substructuring method has been used to reduce the computation time of SPIF simulations using implicit integration [123, 145]. This involves dividing the FE mesh in regions with different computation treatments. The hypothesis is that plastic deformation is localised and restricted to the tool vicinity, while elastic deformation region is considered in the rest of the sheet mesh due to a low geometrical nonlinearity. The strong nonlinearity requires the use of the standard Newton method, but it was not efficient to use in a large elastic deformation part. Using a relatively less expensive iterative procedure, as the modified Newton method, reduces the cost of the tangent stiffness matrix and the internal force vector update at iteration level. The difference between Newton method and the modified Newton method is the treatment of the tangent stiffness matrix [146]. To reduce the computation time, different domain approaches were applied for the treatment of each mesh zones.

6.4 Technology assessment and future guidelines

Simulation efforts have largely focussed on simple geometries such as truncated pyramids and cones, where symmetry can be readily exploited. There is a need to provide rigorous proof of extending the current techniques to more complex parts, where the curvature may change rapidly, leading to alternating regions of under forming and over forming, which may not be very well predicted by simulation. Furthermore, setting up of simulation requires data from experimental tests such as line tests. Typically, these tests need to be specifically done for the particular batch of sheet material that is then used for the parts whose experimental data will be compared to simulation results. This limits the value of simulation as it requires characterization on a regular basis in an industrial setting and also requires using up sheet material, which can be expensive for application alloys such as medical grade titanium. Although simulation times have come down significantly and the process is now better understood, regression based models do it significantly faster (minutes compared to several hours using simulation for nominal sized models) and hence, there is still room for significant improvement. The prediction of failure using simulation models has only been achieved to a limited extent and improved constitutive laws are needed to achieve the same. Future work needs to focus on improving current limitations in simulation time, prediction of accuracy on complex parts, constitutive laws and failure prediction.

7. Sustainability of SPIF

7.1 Effects of process parameters on sustainability

Aspects of environment friendliness of the incremental forming process have been studied lately. Some of this work is focused on the analysis of minimum work required to form the sheet. The theoretical work is an early energy indicator which actually represents a lower bound of the actual electric energy consumption. In an early work, Ingarao et al. [147] developed a comparative analysis between SPIF and conventional deep drawing processes. The processes were analyzed with respect to the quantification of minimum work required to form the sheet and material use in each one. The comparison was developed with varying three processes parameters: two different material strengths (AA-1050 and AA-5754), two different thicknesses (1 mm and 1.5 mm) and two different shapes (truncated cones and truncated pyramids). For each process, therefore, eight different process parameter configurations were tested. The results showed that SPIF requires a higher amount of energy which in part is compensated by the absence of dies in the process.

Comparative analysis was completed by an estimation of potential material saving. The difference in deformation mechanics between the considered processes causes different material use. It was found that SPIF enables a material saving as high as 10 % compared to conventional deep drawing approaches. Earlier, Anghinelli et al. [148] included in the analysis the theoretical energy for cutting off (after the SPIF processes) the area of the sheet used for clamping the starting blank. In this paper different lubricants and different methods were applied to account for the impact of lubrication.

Li et al. [149] analyzed the impact of several process parameters on deformation energy and shape accuracy. They used response surface methodology coupled with multi-objective optimization techniques to analyze the influence of 5 factors: step down, sheet thickness, tool diameter and wall angle at three levels using a Box-Behnken design of experiments. The authors found that deformation energy heavily depended on the sheet thickness and increasing step-down size or decreasing the wall angle was an effective approach to reduce the deformation energy. Even though the analysis still concerned the theoretical minimum work required to form the sheet, this work represented an effort to consider both environmental and technical output metrics. This research suggested that multi-objective approach design could be a suitable way to go to properly take into account all the design objectives (technical, economic and environmental).

Other studies instead have a wider perspective as they take into account more factors of influence. Branker et al. [150] carried out studies on how energy consumption, CO₂ emissions and costs can be studied for SPIF. In this paper, an initial analysis of cost, energy and carbon dioxide (CO₂) emissions that occur in producing a unique aluminum hat using single point incremental forming (SPIF) was performed. A unique hat from Al-3003 O was formed using a Bridgeport GX 480 vertical mill. Two different scenarios were analyzed: the second scenario involved doubling the feed rate and step down increment of the first scenario, as well as using an eco-benign lubricant. The paper offers a preliminary study about the impact of forming time on the energy consumption. The contribution of non-productive times (idle times) in working cycle energy consumption was also discussed. The total electric energy consumed by SPIF processes significantly decreases as the forming time decreases. Besides the electrical energy consumption the paper takes into account the environmental impact of other factors of influence viz.: lubricant, material and tooling. The authors state electrical energy is the second largest contributor of CO₂ emissions for SPIF processes. They also report that the used machine tool was not efficient as the contribution of ancillary energy is relevant and in consequence the overall process efficiency is very low. In this study, it was shown that an eco-benign lubricant derived from used cooking oil could be used in SPIF enabling a certain environmental impact reduction.

7.2 Comparative studies on different setups

The concept of exergy analysis was used to study two ISF technologies (single sided and double sided incremental forming) and compared with conventional forming and hydroforming [151]. It was concluded that ISF is environmentally advantageous for prototyping and small production runs. The incremental forming set up was based on two hexapods with 6 degree of freedom each. Six case studies were studied by combining three different shapes (box, cone and dome) and two different materials: aluminum alloy AA-6022 and Deep Drawing Quality (DDQ). The authors point out that over the entire forming process, approximately just 16 – 22% of the total electric energy input is caused by the tool displacement and forming while the remainder of the electrical energy consumption is ascribable to the idle running (controller, power supply, relays etc.) The process efficiency was evaluated to be 1% and 0.8% with single point incremental forming and doubled sided incremental forming respectively. The results from these studies also revealed that incremental forming processes is advantageous for small production runs up to 300 parts from an environmental perspective. Some potential process improvements were suggested such as using less lubricant, reduction of electricity input by both reducing the consumption for idle running and reducing the forming time.

Studies on electric energy consumption have been the focus of some studies. Bagudanch et al. [152] measured the energy consumption of a Kondia HS1000 3-axis milling machine used for SPIF. 24 experiments were carried out by varying 3 sheet materials, 2 thicknesses, 2 depth steps and 2 spindle speeds. The authors concluded that among the process parameters analyzed, spindle speed was the most influential. A comprehensive electric energetic analysis of single point incremental forming processes was presented by

Ingarao et al. [153, 154]. In this study, the three most commonly used machine tool architectures, a CNC milling machine, a six axis robot and a dedicated AMINO machine tool used for SPIF were considered. A working cycle time study and a power study were carried out. For each set-up the impact of productive as well as of non-productive production modes was analyzed; in addition, the contribution of each sub-unit in the machine architecture towards the total energy demand was studied. The influence of the most relevant process parameters (sheet material strength, feed rate and step down) was analyzed. For the six axes robot, the influence of the sheet positioning was also studied. The study conclude that the energy demand of SPIF processes can be reduced by decreasing the forming time by optimizing the toolpath and working at the highest admissible feed rate. The power consumption of the CNC machine tool did not vary with material. The six-axis robot proved to be sensitive to the material being formed. The so-called material contribution share on the total energy demand accounted for up to 22% for the material with the highest tensile strength in the considered materials set.

It was also found that the CNC milling machine was characterized by a low machine tool efficiency. The AMINO setup provided best results when the instantaneous power demand was considered, but when considering the total energy demand, the robot provided the best solution. This is due to the fact that the robot allows higher speeds which leads to shorter forming times and, in consequence, leads to lower total electric energy usage. The obtained comparative results are reported in Table 4.

Table 4. Electrical energy performance of the most used SPIF platforms

SPIF platform	Forming Time [s]	Average Power Level [W]	Additional energy[%]
CNC milling machine	430	2825	563%
AMINO	588	379	23%
Robot	287	181	Reference

As discussed earlier, two relevant drawbacks still limit the industrial application of SPIF: geometrical accuracy and slow process. Some authors tried to overcome such issue by introducing the idea of high-speed incremental sheet forming (ISF) [36, 155]. By reducing the time required to form parts, the process can be made more environment friendly due to reduced energy consumption. These issues were considered in recent work [156] by comparing the energy consumption of SPIF processes of two different setups: traditional SPIF processes developed on a CNC milling machine and high speed incremental forming developed on a CNC lathe. Experiments were carried out on a vertical milling machine Mazak Nexus 410 A(4-axis CNC work centre), while for the high speed incremental forming set up a MazakTM QTurn 1000 CNC lathe was used. The experimental study was aimed at manufacturing a truncated cone made of 1mm thick AA-5754 aluminum alloy sheets. For each set up 2 two different parameters setting were analyzed, in particular two different feed rate values were tested while all the remaining process parameters have been kept unchanged. A forming time reduction from 420 s (traditional setup) to 12 s (high speed set up) was observed. Such time reduction led to relevant energy saving: from 1333.0 kJ for the CNC machine to 103.6 kJ for the high speed setup.

In recent work, Bagudanch et al. [157, 158] have looked at electric energy consumption and temperature variations while forming polymers. Two polymeric materials (polycarbonate (PC) and polyvinylchloride (PVC)) were used for this study. A design of experiments was used to study the effect of step down, tool diameter, feed rate, spindle speed, sheet thickness on outputs such as energy, temperature, forces, final depth and surface roughness. A typical power consumption profile from these tests is shown in Fig. 16. The authors concluded that by setting the most suitable process parameters, it is possible to minimize the energy consumption and the economic cost of running the process to manufacture polymeric parts.

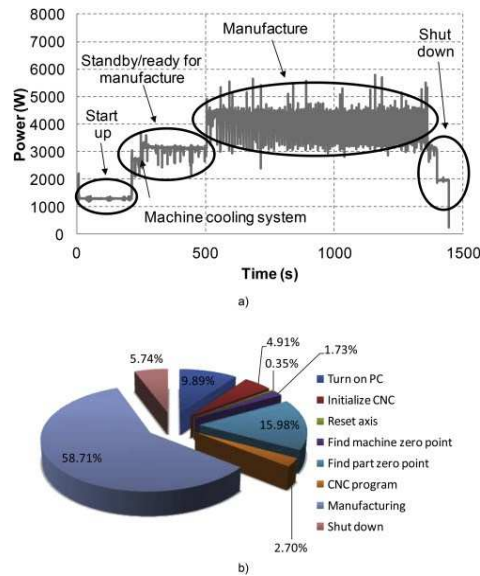


Fig.16. Power consumption profile for SPIF tests [157] [with permission from publisher]

7.3 Technology assessment and future guidelines

In summary, many studies demonstrated that electric energy consumption during forming time is the dominant factor in the energy demand of SPIF processes. In consequence, the first strategy to reduce the energy demand of SPIF processes is reducing the forming time by optimizing the toolpath and working at the highest admissible feed rates. Other researchers demonstrated that SPIF is a green choice when small batch size have to be manufactured, otherwise conventional stamping processes are more efficient. On the other hand, SPIF processes might lead to some material savings. Incremental forming processes enable a material saving as high as 10 % with respect to conventional deep drawing approaches. Overall it is possible to state that the machine tools efficiency is very low. Poor performance is mainly due to the use of non-dedicated machine tools to perform SPIF. It is necessary to underline that the CNC milling machine is not a SPIF dedicated machine tool: the loads required by incremental forming processes are much lower than the ones required for machining processes for which these machine tools are designed. Therefore, the operational power level is very high and the machine tool efficiency is unsatisfactory. Studies revealed that an inappropriate choice of platform can dramatically worsen the energy efficiency and ultimately the total environmental impact of a given process. On the contrary, proper machine tools selection coupled with environmental conscious process parameters selection could result in strong electric energy reductions. Some improvement measures could be implemented at machine tool level to reduce electric energy consumption: proper selection and use (e.g. near to their maximum capacity) of machine tools within a process, machine tools architecture optimization and selective actuation of sub-units.

8. Applications

Over the last 10 years, the application areas of incremental forming have expanded beyond the initial suggestions in the structured search carried out by Allwood et al. [159] to include medical implants, product prototyping, architecture, automotive, dies and molds, aerospace and transportation. Table 5 includes a summary of these applications with a number of them using metallic alloys and a few involving polymers. Some of these applications are discussed below.

Table 5. Applications of incremental forming

Application area	Year	Authors	Application	Material
Medical	2005	Ambrogio et al. [160]	Ankle support	DDQ steel
	2005	Duflou et al. [161]	Cranial plate	AA 3003-O
	2010	Oleksik et al. [162]	Knee implant	Pure Ti
	2011	Fiorentino et al. [163]	Palate prosthesis	Polycaprolactone (PCL), Ti grade 2
	2012	Fiorentino et al. [164]	Cranial plate	Ti grade 2

	2012	Eksteen et al. [165, 166]	Knee prosthesis	Ti grade 2
	2013	Behera et al. [167]	Cranial plate	Ti grade 2
	2015	Behera et al. [14]	Cranial plate	Ti grade 1
	2015	Bagudanch et al. [168]	Cranial plate	PCL
	2013	Behera et al. [60]	Backseat orthosis	AA 3103
	2014	Araújo et al. [13]	Facial implant	Ti grade 2
Architectural	2008	Jackson et al. [18]	Sandwich panel	Multiple
Forming equipment	2006	Allwood et al. [169]	Dies and molds	Al alloy
	2013	Appermont et al. [170]	Dies and molds	DC01, AA 3103
Automotive	2007	Governale et al. [171]	Car body	Al alloy
	2010	Verbert et al. [43]	Car fender	AA 3103
	2009	Bambach et al. [78]	Car fender	DC04
Transportation	2013	Junchao et al. [172]	Car tail light	DC04
	2009	--	Shinkansen (Bullet Train)	--
Aerospace	2013	Behera et al. [10]	Airfoils	AA 5754

8.1 Medical implants

Medical implants have been one of the most researched applications of SPIF due to the need for customization to the shape of the human body. Specific applications have included ankle support, cranial plate, palate prosthesis, knee prosthesis, backseat prosthesis and facial implant. Titanium has been one of the key materials formed in these studies and both grade 1 [14] and grade 2 [167] have been tried out. Bio-polymers such as polycaprolactone [163, 168] and nano-polymer composites [173] have also been experimented with. Detailed experimental studies on polymeric cranial implants have opened the possibility of clinical applications [174, 175]. One of the key challenges has been to address the need for achieving high forming angles for freeform shapes while also meeting the desired accuracy specifications. The use of mesh morphing techniques [11] has shown considerable promise in meeting this dual requirement, while compensation for freeform features has been realized by using ellipsoidal training sets to generate accuracy response surfaces [14]. Fig. 17 shows a successful attempt of forming with enhanced accuracy using a mixed regression model that uses principal curvatures for combining accuracy responses surfaces from ruled and freeform features [14].

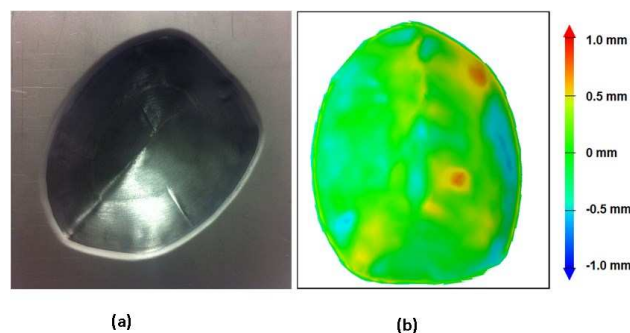


Fig.17. Cranial implant manufactured with a compensated toolpath showing (a) a sample formed part shown in top view and (b) accuracy plot for the compensated part using a mixed MARS model and a compensation factor of 0.7 [14] [with permission from publisher]

8.2 Applications using sandwich panels

The potential use of SPIF for forming sandwich panels to act as 3D shells has been reported by Jackson et al. [18]. Sandwich panels have found applications in aerospace, marine, automotive and civil engineering [176]. For instance, automotive components such as dash panel and inner wheel housing may use these panels [177]. They explored the feasibility of manufacturing these panels by examining failure modes, sheet

thinning and surface quality. This exploratory study concluded that sandwich panels which are ductile and hold largely incompressible cores can be formed using SPIF. The conclusions were based on analysis of tool force, sheet thickness measurements and through thickness deformation analysis that compared the results obtained in sandwich panels with metallic sheets. It was also shown that aluminum foam cores were formable using SPIF. Fig. 18 shows two panels formed using mild steel and aluminium alloy cores.

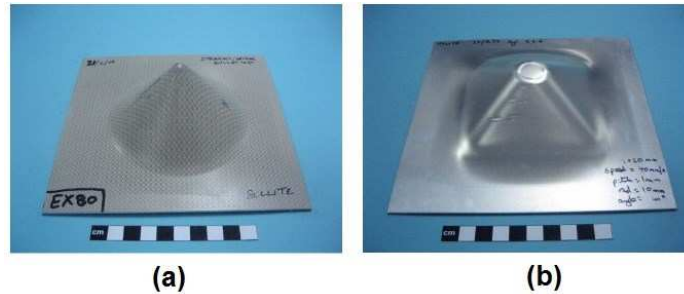


Fig.18. Sandwich panels made by SPIF (a) Sollight with composition of mild steel and polypropylene - MS/PP/MS (45° wall angle formed without failure) and (b) Hylite with composition of aluminium alloy AA 5182 and polypropylene - Al/PP/Al (40° angle showing faceplate fracture) [18] [with permission from publisher]

8.3 Thin sheet molds

Molds are often used to produce parts using thermoforming techniques such as vacuum forming. In vacuum forming, a plastic sheet is first heated and then molded into a thin sheet mold to produce the plastic part. Instead of using a solid block mold made of a single material, it is possible to instead use a thin sheet based mold. The problem with using a thin sheet mold is that it cannot withstand forces during vacuum forming and can buckle or distort. Hence, a work around for this technique has been proposed by Appermont et al. [170] where a mold is built with a thin sheet and a filler material.

Truncated pyramids formed using SPIF were used to create a mold box made of low carbon steel alloy, DC01, with a sheet thickness of 1.5 mm and wall angle 60°. A filler material consisting of expanded clay grains AR-8/16-340 and an acrylic casting resin, ALWA-MOULD D/ATLAS M 130 was used to bind the grains together. The DC01 pyramid used compensation using MARS predictions ensuring high dimensional accuracy with a maximum deviation 0.917 mm and standard deviation 0.463 mm (see accuracy profile in Fig. 19 (a)). A backing plate of size 150 mm was used and a tool of diameter 10 mm was used to form the part. This mold was subjected to vacuum forming, which was successful in forming the plastic part shown in Fig.19 (b).

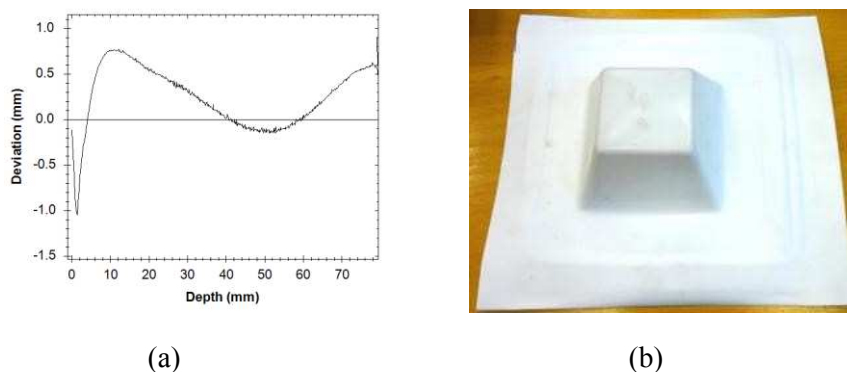


Fig.19.(a) Accuracy plot of DC01 truncated pyramid used as a mold (b) vacuum formed plastic part that used the mold made of DC01 [60]

8.4 Automotive, transportation and aerospace applications

As automotive, transportation and aerospace applications require formed sheet metal components, SPIF has a potential to benefit this sector both during the design phase for parts to be used as prototypes for testing and also for actual use in the final product, particularly where customization is necessary. One of the key

considerations for forming parts for these applications is that the part size is typically larger than the working range of milling machines, which often necessitates the use of robots and consequently, the dimensional accuracies obtained are lower due to the stiffness of the robot. Secondly, a large part size necessitates a longer forming time.

Some examples of attempts made to illustrate this potential has been in the form of car fender parts made by Verbert et al. [43] and Bambach et al. [78], a scaled model of a Japanese Shinkansen bullet train model built by Amino Corporation [178] and scaled airfoils [11]. Intelligent multi-step tool paths have been designed for specific applications such as a taillight bracket for a car made in DC04 of 0.8 mm thickness [172]. Lozano et al. [179] formed the cover of a motorcycle exhaust pipe using both SPIF and two point incremental forming and concluded that the latter resulted in better part accuracy compared to SPIF. Ford has taken up incremental forming for its automotive components and labeled it the Ford Freeform Fabrication Technology (F3T) [180]. Fig. 20 shows the bullet train and a Ford logo made using ISF.



Fig.20. (a) 1/8 scaled model of a Shinkansen bullet train [178] (b) Ford logo using the F3T technology [180] [with permission from publishers]

8.5 Summary

While a number of applications have been investigated over the last decade, the fundamental limitations of SPIF with respect to accuracy, process limits and sheet thickness variations have hampered wide scale industrial use. A summary of achieved accuracies using the latest tool path compensation methods is reported in Table 6. The maximum deviations are below 1 mm for many cases, which is a significant improvement compared to well over 5 mm for parts sized up to 200 mm x 200 mm in 2005. One of the key challenges in commercial applications is that of improving the process outcomes vis-à-vis traditional forming processes. While SPIF reduces the lead time to start forming parts by not requiring custom dies or molds, the process itself is quite slow for large sized applications in certain sectors such as automotive, aerospace and civil engineering. Besides, the new tooling and software based tool path compensation strategies that help improve process outcomes have not been widely applied in industrial application demonstration case studies. It is necessary to generate industry interest leading to more challenging applications, which can in turn improve the understanding of the process, drive a trend towards automation and enhance process outcomes.

Table 6. Some applications for SPIF and realized accuracies [14, 60, 168]

Application	Materials	Sheet thickness	Compensation/ Toolpath strategy	Achieved accuracy (maximum deviation)	Achieved accuracy (average absolute deviation)
Thin sheet molds	AA 1050	1.5	MARS	0.558	0.119
	AA 3103	1.5	Offset MARS [12]	0.570	0.248
	DC01	1.5	MSPIF*	0.772	0.173
	DC01	1,1.5	MARS	0.917	0.396
Cranio-facial implants	AA 1050	1.5	Intermediate shapes + Simple compensation	0.834	0.106
	AISI 304	0.5	Intermediate shapes + Simple compensation	1.721	0.230
	Titanium grade 2	1	Intermediate shapes + Simple compensation	2.019	0.354
	Titanium grade 1	0.5	Freeform MARS	0.570	0.050

	PCL	2.0	Uncompensated	3.766	--
Back seat orthosis	AA 3103	1.5	Reprocessing + DSPIF**	1.229	0.236
Face mask	AA 1050	1.5	DSPIF**+Partial toolpaths	3.333	0.053
Airfoil	AA 5754	1	Offset MARS	0.656	0.323
			Generic error correction function		
			MARS for ruled features		
	AISI 304	0.5	Morphing	0.497	0.317

* *MSPIF – Multi step SPIF*[5]

***DSPIF – Double sided SPIF*[85]

9. Future research topics, roadmap and summary

Incremental forming has come a long way from being considered as a relatively new process with skepticism on the potential applicability in industry, in the CIRP keynote review [3]. The assessment performed then had shown a few key applications which could be potentially harvested and mentioned that SPIF is unlikely to be a direct replacement for an existing manufacturing process. However, the improvements realized in terms of enhanced process limits, control over sheet thickness and improved geometric accuracy have put this technology at the forefront of emerging sheet forming technologies being actively considered for wide spread industrial incorporation. New tooling developments are being realized with the maturing of CNC process technologies, such as Three Opposite Point Incremental Forming (TOPIF), recently proposed by Wang et al. [181]. Simulation capabilities have increased during the last decade and the computational time required to assess formability and geometric accuracy have been reduced from days and weeks to a few hours. New process planning tools are now available with advanced mesh processing capabilities that enable toolpath optimization providing more precise control over the geometric shape.

With the adoption of SPIF by companies such as Ford and Arcelor, the process has a promising future. In addition, current research efforts are directed at harvesting specific applications, particularly related to medical implants and molds and dies. The use of heat assisted forming techniques has also shown significant promise and further research in this direction will help develop constitutive equations for modeling the heat assisted incremental forming processes such as LASPIF and electric hot SPIF, enhancing process limits and improving geometric accuracy further. The initial success in high speed incremental forming at high feed rates has shown promise. However, further investigations are necessary to extend the geometrical shapes to include non axi-symmetric shapes and control the process with regard to process limits, sheet thickness control and geometric accuracy. Initial evidence for ideal operating ranges for different process parameters in SPIF that control formability has been reported and this needs a detailed investigation that could be best done if different research groups working on SPIF can share and exchange detailed process data, as often different techniques are used by different groups to determine formability and the experimental setups and operating process parameters vary widely [182].

Table 7 outlines the current state of the art as it emerged from this review work and suggests future work in the field over the next decade. With emerging applications in multiple sectors, SPIF can be integrated as part of flexible manufacturing systems (FMS) in industries. While a small number of hybrid alternatives such stretch forming combined with SPIF have been explored, complex hybrid processes forming part of multi-technology platforms can be envisaged for the future. It is particularly important to extend the applicability of new tooling approaches such as stiffening elements [183] and develop generic error correction functions that extend to large sized parts and can be tuned as per the machine stiffness, to improve accuracy of formed parts. It may be noted that tooling based alternative process variants such as double sided incremental forming (DSIF) using two tools have shown the promise to improve a number of limitations of SPIF. However, as the hardware for these variants is slightly more complicated, adapting milling machines to carry out the same has not been straightforward and consequently, data on these variants is still limited and necessitates further exploration.

The vision for Industry 4.0 seeks to realize an intelligent future where the internet of things, services and people come together. SPIF can be a contributor to the realization of this vision by closing the current gaps that are evident from this review. The use of real time monitoring systems has become a reality for modern industrial factories and the same needs to be integrated into SPIF research in a larger way than currently where a few experiments involve use of offline digital image correlation or a small amount of online depth accuracy corrections. While a recent work talks about the integration of SPIF into cloud manufacturing platforms [184], the same is yet to be realized. While the strides in simulations for SPIF have been strong, a lot still needs to be done if we are to achieve accurate predictions for failure location and spring back

prediction in complex parts that have a multitude of features. Improved constitutive laws will go a long way in realizing the same and these need to encompass the emerging hybrid processes as well. Sustainability research in SPIF is still in an early stage and novel machine tool and process designs that reduce scrap in the process need to be forthcoming. Additionally, the applications base can be enlarged to encompass new areas as outlined in Table 7, thereby engaging industrial partners from different technological areas.

Table 7. Roadmap for next 10 years: outline of state of the art and potential future work on SPIF

Review area	Current state of the art	Future work potential
Hardware requirements	<ul style="list-style-type: none"> •Adapted machines and/or purpose built solely for SPIF operations •Hybrid processes (simple designs) 	<ul style="list-style-type: none"> •SPIF as part of flexible manufacturing systems (FMS)/ supply chain that includes subtractive, additive and other manufacturing techniques •Complex hybrid processes that include SPIF •Integrating with real time communication systems as part of Industry 4.0 implementation
Formability/ Failure limits	<ul style="list-style-type: none"> •Improved limits using multi-step, heat supported strategies, control of process parameters such as step down, tool diameter, etc. 	<ul style="list-style-type: none"> •Improved failure prediction (precise wall angle, depth) using better constitutive models •Hybrid processes that use other processes for steep wall angle areas
Forces	<ul style="list-style-type: none"> •Force models with < 15 % error e.g. Aeren's model •Optimized toolpaths to reduce forces 	<ul style="list-style-type: none"> •Fast force simulation algorithms/ in-situ systems for force controls
Toolpath strategies	<ul style="list-style-type: none"> •Contouring, helical, multi-step, double sided, mixed (in to out with out to in) •Springback compensation for parts made on milling machines (limited by size) 	<ul style="list-style-type: none"> •Real time monitoring systems (e.g. vision systems) with live toolpath correction strategies
Accuracy	<ul style="list-style-type: none"> •Feature based compensation •Regression based predictions •Local geometry matrix based predictions •Graph topological approaches 	<ul style="list-style-type: none"> •Tooling approaches (e.g. stiffening elements) to improve process limits •Generic error correction functions that extend to large sized parts
Sheet thickness variations	<ul style="list-style-type: none"> •Sequential limit analysis based predictions •Limited tool path based control •Kinematics models 	<ul style="list-style-type: none"> •Optimized multi-step strategies for thickness control using FE predictions •Multi axis tooling and optimized work piece orientation working in sync with mathematical models to control thickness precisely
Simulation	<ul style="list-style-type: none"> •Fast simulation, remeshing techniques •Limited failure prediction capabilities – specific cases but not extended generically to wide range of sheet materials, geometries, thicknesses and process parameters •Geometric accuracy and force predictions for simple shapes – two slope truncated pyramids and cones 	<ul style="list-style-type: none"> •Improved constitutive laws reflecting bending-stretching mechanics better •Extend simulation capabilities to wide range of sheet materials, geometries, thicknesses and process parameters •Enhanced failure and accuracy prediction •Accurate and fast simulation of process variants (e.g. heat supported SPIF, multi step SPIF) for specific process outcomes
Sustainability	<ul style="list-style-type: none"> •Early quantitative and comparative work on energy consumption in SPIF on different setups such as milling machines, robots, Amino etc. 	<ul style="list-style-type: none"> •Analytical models for accurate environment impact estimation •Comparative analyses to identify production scenarios where SPIF is preferable to other forming processes •Waste/scrap reduction in SPIF operations e.g.: production of tunnel-type parts, instead of container-type parts
Applications	<ul style="list-style-type: none"> •Obsolete applications facing stiff competition from additive manufacturing alternatives 	<ul style="list-style-type: none"> •Extend initial work on molds to assist other manufacturing processes such as rotational forming •Repair and maintenance of thin sheet parts in automotive and aerospace sectors •Architectural and civil engineering applications •Restoration of archaeological artefacts

A systematic assessment to cover the last 10 years of developments in SPIF was carried out in this study. Key hardware developments have been summarized and this provides the direction for futuristic setups, which can include multi axis machine tools capabilities. Parallel kinematics have shown promise and stiffer robots are being developed, which can be used for SPIF. Compensation for low stiffness and chatter on

robots can be combined with optimized mixed tool path strategies which take into account spring back and sheet anisotropy to provide a step change in accuracy limitations. The process fundamentals in terms of forming mechanics, forces, tool paths and thickness variations were systematically mapped in this study. This was followed by discussion on the efforts to overcome the limitations of SPIF in terms of process windows and geometric accuracy. The work on simulation has been carefully surveyed and the improvements in computational cost have been highlighted. In addition, a much neglected area of process sustainability has been covered as a fundamental departure from the keynote review done in 2005. Applications of SPIF, which have increased in significant numbers, over the last decade have been tracked and this should provide the guidance for the development of industrial flexible forming systems based on SPIF.

Acknowledgements

The authors would like to thank funding agencies which have sponsored research in incremental forming including Fonds Wetenschappelijk Onderzoek (FWO, Belgium), Fundação para a Ciência e a Tecnologia (FCT, Portugal), Romania Ministry of Education and Research, National University Research Council, Romania and Engineering and Physical Sciences Research Council (EPSRC, UK). The authors also thank José I. V. Sena, Bin Lu, Hengan Ou, Joost Duflou, Robertt Valente, Philip Eyckens, Carlos F. Guzman and Anne-Marie Habraken for invaluable discussions without which this paper would not have been possible.

References

- [1] J. Verbert, A.K. Behera, B. Lauwers, J.R. Duflou, Multivariate Adaptive Regression Splines as a Tool to Improve the Accuracy of Parts Produced by FSPIF, *Key Eng Mater*, 473 (2011) 841-846.
- [2] E. Leszak, Apparatus and process for incremental dieless forming, in: Patent US3342051A, , 1967.
- [3] J. Jeswiet, F. Micari, G. Hirt, A. Bramley, J. Duflou, J. Allwood, Asymmetric single point incremental forming of sheet metal, *Cirp Ann-Manuf Techn*, 54 (2005) 623-649.
- [4] S. Marabuto, D. Afonso, J. Ferreira, F. Melo, M.A. Martins, R. de Sousa, Finding the Best Machine for SPIF Operations-a Brief Discussion, in: *Key Engineering Materials, Trans Tech Publ*, 2011, pp. 861-868.
- [5] J.R. Duflou, J. Verbert, B. Belkassen, J. Gu, H. Sol, C. Henrard, A.M. Habraken, Process window enhancement for single point incremental forming through multi-step toolpaths, *Cirp Ann-Manuf Techn*, 57 (2008) 253-256.
- [6] R. Malhotra, L. Xue, T. Belytschko, J. Cao, Mechanics of fracture in single point incremental forming, *Journal of Materials Processing Technology*, 212 (2012) 1573-1590.
- [7] Y. Fang, B. Lu, J. Chen, D. Xu, H. Ou, Analytical and experimental investigations on deformation mechanism and fracture behavior in single point incremental forming, *Journal of Materials Processing Technology*, 214 (2014) 1503-1515.
- [8] C. Henrard, C. Bouffioux, P. Eyckens, H. Sol, J. Duflou, P. Van Houtte, A. Van Bael, L. Duchêne, A. Habraken, Forming forces in single point incremental forming: prediction by finite element simulations, validation and sensitivity, *Computational mechanics*, 47 (2011) 573-590.
- [9] L. Duchêne, C.F. Guzmán, A.K. Behera, J.R. Duflou, A.M. Habraken, Numerical simulation of a pyramid steel sheet formed by single point incremental forming using solid-shell finite elements, in: *Key Engineering Materials, Trans Tech Publ*, 2013, pp. 180-188.
- [10] A.K. Behera, B. Lauwers, J.R. Duflou, Tool path generation framework for accurate manufacture of complex 3D sheet metal parts using single point incremental forming, *Comput Ind*, 65 (2014) 563-584.
- [11] A.K. Behera, B. Lauwers, J.R. Duflou, Tool path Generation for Single Point Incremental Forming using Intelligent Sequencing and Multi-step Mesh Morphing Techniques, *Key Eng Mater*, 554-557 (2013), pp. 1408-1418
- [12] A.K. Behera, J. Verbert, B. Lauwers, J.R. Duflou, Tool path compensation strategies for single point incremental sheet forming using multivariate adaptive regression splines, *Comput Aided Design*, 45 (2013) 575-590.
- [13] R. Araujo, P. Teixeira, L. Montanari, A. Reis, M.B. Silva, P.A. Martins, Single point incremental forming of a facial implant, *Prosthetics and orthotics international*, 38 (2014) 369-378.
- [14] A.K. Behera, B. Lu, H. Ou, Characterization of shape and dimensional accuracy of incrementally formed titanium sheet parts with intermediate curvatures between two feature types, *Int J Adv Manuf Technol*, 83:5 (2016) 1099-1111.
- [15] K. Essa, P. Hartley, An assessment of various process strategies for improving precision in single point incremental forming, *Int J Mater Form*, 4 (2011) 401-412.
- [16] P. Martins, L. Kwiatkowski, V. Franzen, A. Tekkaya, M. Kleiner, Single point incremental forming of polymers, *Cirp Ann-Manuf Techn*, 58 (2009) 229-232.
- [17] M. Silva, L. Alves, P. Martins, Single point incremental forming of PVC: Experimental findings and theoretical interpretation, *European Journal of Mechanics-A/Solids*, 29 (2010) 557-566
- [18] K. Jackson, J. Allwood, M. Landert, Incremental forming of sandwich panels, *Journal of Materials Processing Technology*, 204 (2008) 290-303.
- [19] A. Mohammadi, H. Vanhove, M. Attisano, G. Ambrogio, J.R. Duflou, Single point incremental forming of shape memory polymer foam, in: *MATEC Web of Conferences, EDP Sciences*, 2015, 04007
- [20] B. Lu, J. Chen, H. Ou, J. Cao, Feature-based tool path generation approach for incremental sheet forming process, *Journal of Materials Processing Technology*, 213 (2013) 1221-1233.
- [21] J. Jeswiet, D. Adams, M. Doolan, T. McNulty, P. Gupta, Single point and asymmetric incremental forming, *Advances in Manufacturing*, 3 (2015) 253-262.
- [22] S. Gatea, H. Ou, G. McCartney, Review on the influence of process parameters in incremental sheet forming, *Int J Adv Manuf Technol*, (2016) 1-21. doi:10.1007/s00170-00016-08426-00176.
- [23] D. Nimbalkar, V. Nandedkar, Review of incremental forming of sheet metal components, *Int J Eng Res Appl*, 3 (2013) 39-51.
- [24] S. Echraf, M. Hrairi, Research and progress in incremental sheet forming processes, *Materials and Manufacturing Processes*, 26 (2011) 1404-1414
- [25] W. Emmens, G. Sebastiani, A. Van den Boogaard, The technology of incremental sheet forming—a brief review of the history, *Journal of Materials Processing Technology*, 210 (2010) 981-997

- [26] R.A. de Sousa, J. Ferreira, J.S. de Farias, J. Torrão, D. Afonso, M. Martins, SPIF-A: on the development of a new concept of incremental forming machine, *Structural Engineering and Mechanics*, 49 (2014) 645-660.
- [27] J. Verbert, R. Aerens, H. Vanhove, E. Aertbeliën, J.R. Dufloy, Obtainable accuracies and compensation strategies for robot supported spif, in: *Key Engineering Materials*, Key Engineering Materials, 410 (2009) 679-687.
- [28] V.T. Portman, Stiffness evaluation of machines and robots: minimum collinear stiffness value approach, *Journal of Mechanisms and Robotics*, 3 (2011) 011015.
- [29] J. Allwood, N. Houghton, K. Jackson, The design of an incremental sheet forming machine, *Advanced Materials Research*, 6 (2005) 471-478.
- [30] N. Okada, G. Ro, Y. Suzuki, Method and apparatus for incremental forming, in, US Patent 6,971,256 B2, 2005.
- [31] T. Schafer, R.D. Schraft, Incremental sheet metal forming by industrial robots, *Rapid Prototyping Journal*, 11 (2005) 278-286.
- [32] J.R. Dufloy, B. Callebaut, J. Verbert, H. De Baerdemaeker, Laser assisted incremental forming: Formability and accuracy improvement, *Cirp Ann-Manuf Techn*, 56 (2007) 273-276.
- [33] H. Meier, O. Dewald, J. Zhang, A new robot-based sheet metal forming process, in: *Advanced Materials Research*, Trans Tech Publ, 2005, pp. 465-470.
- [34] L. Lamminen, Incremental Sheet Forming with an Industrial Robot—Forming Limits and Their Effect on Component Design, *Advanced Materials Research*, 6 (2005) 457-464.
- [35] M. Callegari, D. Amodio, E. Ceretti, C. Giardini, Sheet incremental forming: advantages of robotised cells vs. CNC machines, *Industrial Robotics: Programming, Simulation and Applications*, (2007) 493-514.
- [36] G. Ambrogio, F. Gagliardi, S. Bruschi, L. Filice, On the high-speed Single Point Incremental Forming of titanium alloys, *Cirp Ann-Manuf Techn*, 62 (2013) 243-246.
- [37] H. Vanhove, A. Mohammadi, Y.S. Guo, J.R. Dufloy, High-Speed Single Point Incremental Forming of an Automotive Aluminium Alloy, in: *Key Engineering Materials*, 622 (2014) 433-439.
- [38] K. Hamilton, J. Jeswiet, Single point incremental forming at high feed rates and rotational speeds: Surface and structural consequences, *Cirp Ann-Manuf Techn*, 59 (2010) 311-314.
- [39] R.N.P. Bastos, R.J.A. de Sousa, J.A.F. Ferreira, Enhancing time efficiency on single point incremental forming processes, *Int J Mater Form*, 9 (2015) 653-662.
- [40] J. Dufloy, B. Callebaut, J. Verbert, H. De Baerdemaeker, Improved SPIF performance through dynamic local heating, *International Journal of Machine Tools and Manufacture*, 48 (2008) 543-549.
- [41] M. Ham, B.M. Powers, J. Loisel, Surface Topography from Single Point Incremental Forming using an Acetal Tool, *Key Engineering Materials*, 549 (2013) 84-91.
- [42] X. Ziran, L. Gao, G. Hussain, Z. Cui, The performance of flat end and hemispherical end tools in single-point incremental forming, *Int J Adv Manuf Technol*, 46 (2010) 1113-1118.
- [43] J. Verbert, Computer Aided Process Planning for Rapid Prototyping With Incremental Sheet Forming Techniques, PhD Thesis. Katholieke Universiteit Leuven, Leuven, 2010.
- [44] B. Callebaut, J. Dufloy, J. Verbert, Asymmetric incremental sheet forming system, US Patent US20090158805, 2011.
- [45] T. Obikawa, S. Satou, T. Hakutani, Dieless incremental micro-forming of miniature shell objects of aluminum foils, *International Journal of Machine Tools and Manufacture*, 49 (2009) 906-915.
- [46] T. Obikawa, T. Sekine, Fabrication of Miniature Shell Structures of Stainless Steel Foil and Their Forming Limit in Single Point Incremental Microforming, *International Journal of Automation Technology*, 7 (2013) 256-262.
- [47] J. Brüninghaus, Y. Volfson, J. Bickendorf, S. Brell-Cokcan, Design of a Novel End-Effector for Kinematic Support in Incremental Sheet Forming, *Key Engineering Materials*, 716 (2016) 395-401.
- [48] J. Jeswiet, D. Young, Forming limit diagrams for single-point incremental forming of aluminium sheet, *Proceedings of the Institution of Mechanical Engineers, Part B: Journal of Engineering Manufacture*, 219 (2005) 359-364.
- [49] G. Hussain, L. Gao, N. Hayat, L. Qijian, The effect of variation in the curvature of part on the formability in incremental forming: An experimental investigation, *International Journal of Machine Tools and Manufacture*, 47 (2007) 2177-2181.
- [50] L. Filice, G. Ambrogio, F. Micari, On-line control of single point incremental forming operations through punch force monitoring, *Cirp Ann-Manuf Techn*, 55 (2006) 245-248.
- [51] R. Aerens, P. Eyckens, A. Van Bael, J. Dufloy, Force prediction for single point incremental forming deduced from experimental and FEM observations, *Int J Adv Manuf Technol*, 46 (2010) 969-982.
- [52] A. Szekeres, M. Ham, J. Jeswiet, Force measurement in pyramid shaped parts with a spindle mounted force sensor, *Key Engineering Materials*, 344 (2007), pp. 551-558.
- [53] G. Hussain, L. Gao, N. Hayat, X. Ziran, A new formability indicator in single point incremental forming, *Journal of Materials Processing Technology*, 209 (2009) 4237-4242.
- [54] P. Eyckens, Formability in Incremental Sheet Forming: Generalization of the Marciniak-Kuczynski Model, PhD Thesis. KU Leuven, Leuven, 2010.
- [55] G. Centeno, I. Bagudanch, A.J. Martínez-Donaire, M.L. Garcia-Romeu, C. Vallengano, Critical analysis of necking and fracture limit strains and forming forces in single-point incremental forming, *Mater Design*, 63 (2014), pp. 20-29.
- [56] J. Velosa De Sena, Advanced numerical framework to simulate Incremental Forming Processes, PhD Dissertation. Université de Liège and University of Aveiro, 2015.
- [57] W.C. Emmens, A. Van den Boogaard, Strain in shear, and material behaviour in incremental forming, *Key Engineering Materials*, Trans Tech Publ, 344 (2007), 519-526.
- [58] W. Emmens, A. Van den Boogaard, An overview of stabilizing deformation mechanisms in incremental sheet forming, *Journal of Materials Processing Technology*, 209 (2009) 3688-3695.
- [59] M. Silva, M. Skjoldt, P.A. Martins, N. Bay, Revisiting the fundamentals of single point incremental forming by means of membrane analysis, *International Journal of Machine Tools and Manufacture*, 48 (2008) 73-83.
- [60] A.K. Behera, Shape Feature Taxonomy Development for Toolpath Optimisation in Incremental Sheet Forming, PhD Thesis. Katholieke Universiteit Leuven, 2013.
- [61] L. Fratini, G. Ambrogio, R. Di Lorenzo, L. Filice, F. Micari, Influence of mechanical properties of the sheet material on formability in single point incremental forming, *Cirp Ann-Manuf Techn*, 53 (2004) 207-210.
- [62] P. Martins, N. Bay, M. Skjoldt, M. Silva, Theory of single point incremental forming, *Cirp Ann-Manuf Techn*, 57 (2008) 247-252.
- [63] K. Jackson, J. Allwood, The mechanics of incremental sheet forming, *Journal of materials processing technology*, 209 (2009) 1158-1174.
- [64] P. Eyckens, B. Belkassam, C. Henrard, J. Gu, H. Sol, A.M. Habraken, J.R. Dufloy, A. Van Bael, P. Van Houtte, Strain evolution in the single point incremental forming process: digital image correlation measurement and finite element prediction, *Int J Mater Form*, 4 (2011) 55-71.
- [65] P. Eyckens, A. Van Bael, P. Van Houtte, Marciniak-Kuczynski type modelling of the effect of through-thickness shear on the forming limits of sheet metal, *International Journal of Plasticity*, 25 (2009) 2249-2268.
- [66] P. Eyckens, A. Van Bael, P. Van Houtte, An extended Marciniak-Kuczynski model for anisotropic sheet subjected to monotonic strain paths with through-thickness shear, *International Journal of Plasticity*, 27 (2011) 1577-1597.

- [67] P. Eyckens, S. He, A. Van Bael, P. Van Houtte, J. Dufloy, Forming limit predictions for the serrated strain paths in single point incremental sheet forming, in: Proceedings of the 9th International Conference on Numerical Methods in Industrial Forming Processes NUMIFORM'07, AIP Publishing, 2007, pp. 141-146.
- [68] P. Eyckens, J.D.-l. Moreau, J.R. Dufloy, A. Van Bael, P. Van Houtte, MK modelling of sheet formability in the incremental sheet forming process, taking into account through-thickness shear, *Int J Mater Form*, 2 (2009) 379-382.
- [69] P. Eyckens, A. Van Bael, R. Aerens, J. Dufloy, P. Van Houtte, Small-scale finite element modelling of the plastic deformation zone in the incremental forming process, *Int J Mater Form*, 1 (2008) 1159-1162.
- [70] J. Allwood, D. Shouler, A.E. Tekkaya, The increased forming limits of incremental sheet forming processes, *Key Engineering Materials*, 344 (2007), 621-628.
- [71] S. Gatea, B. Lu, H. Ou, G. McCartney, Numerical simulation and experimental investigation of ductile fracture in SPIF using modified GTN model, in: MATEC Web of Conferences, EDP Sciences, 2015, pp. 04013.
- [72] R. Aerens, J. Dufloy, P. Eyckens, A. Van Bael, Advances in force modelling for SPIF, *Int J Mater Form*, 2 (2009) 25-28.
- [73] J.R. Dufloy, Y. Tunckol, R. Aerens, Force analysis for single point incremental forming, *Key Engineering Materials*, 344 (2007), 543-550.
- [74] R. Pérez-Santiago, I. Bagudanch, M.L. García-Romeu, Force modeling in single point incremental forming of variable wall angle components, *Key Engineering Materials*, 473 (2011), 833-840.
- [75] M.J. Mirnia, B.M. Dariani, Analysis of incremental sheet metal forming using the upper-bound approach, Proceedings of the Institution of Mechanical Engineers, Part B: Journal of Engineering Manufacture, (2012) 0954405412445113.
- [76] Y. Li, W.J. Daniel, Z. Liu, H. Lu, P.A. Meehan, Deformation mechanics and efficient force prediction in single point incremental forming, *Journal of Materials Processing Technology*, 221 (2015) 100-111.
- [77] M. Skjødt, M.H. Hancock, N. Bay, Creating helical tool paths for single point incremental forming, *Key Eng Mat*, 344 (2007) 583-590.
- [78] M. Bambach, B.T. Araghi, G. Hirt, Strategies to improve the geometric accuracy in asymmetric single point incremental forming, *Production Engineering*, 3 (2009) 145-156.
- [79] J. Dufloy, B. Lauwers, J. Verbert, Y. Tunckol, H. De Baerdemaeker, Achievable accuracy in single point incremental forming: case studies, in: Proceedings of the 8th European Scientific Association for material Forming Conference on Material Forming, 2005, pp. 675-678.
- [80] M. Rauch, J.Y. Hascoet, J.C. Hamann, Y. Plenel, Tool path programming optimization for incremental sheet forming applications, *Comput Aided Design*, 41 (2009) 877-885.
- [81] M. Skjødt, N. Bay, B. Endelt, G. Ingarao, Multi stage strategies for single point incremental forming of a cup, *Int J Mater Form*, 1 (2008) 1199-1202.
- [82] F. Micari, G. Ambrogio, L. Filice, Shape and dimensional accuracy in Single Point Incremental Forming: State of the art and future trends, *Journal of Materials Processing Technology*, 191 (2007) 390-395.
- [83] G. Ambrogio, V. Cozza, L. Filice, F. Micari, An analytical model for improving precision in single point incremental forming, *Journal of Materials Processing Technology*, 191 (2007) 92-95.
- [84] G. Ambrogio, I. Costantino, L. De Napoli, L. Filice, L. Fratini, M. Muzzupappa, Influence of some relevant process parameters on the dimensional accuracy in incremental forming: a numerical and experimental investigation, *Journal of Materials Processing Technology*, 153 (2004) 501-507.
- [85] G. Ambrogio, L. De Napoli, L. Filice, A novel approach based on multiple back-drawing incremental forming to reduce geometry deviation, *Int J Mater Form*, 2 (2009) 9-12.
- [86] G. Ambrogio, L. Filice, On the use of Back-drawing Incremental Forming (BIF) to improve geometrical accuracy in sheet metal parts, *Int J Mater Form*, 5 (2012) 269-274.
- [87] G. Ambrogio, L. Filice, G. Manco, Considerations on the incremental forming of deep geometries, *Int J Mater Form*, 1 (2008) 1143-1146.
- [88] A.K. Behera, J. Gu, B. Lauwers, J.R. Dufloy, Influence of Material Properties on Accuracy Response Surfaces in Single Point Incremental Forming, *Key Eng Mater*, 504-506 (2012) 919-924.
- [89] A.K. Behera, B. Lauwers, J.R. Dufloy, An Integrated Approach to Accurate Part Manufacture in Single Point Incremental Forming using Feature Based Graph Topology, *Key Eng Mater*, 504-506 (2012) 869-876.
- [90] A.K. Behera, B. Lauwers, J.R. Dufloy, Advanced feature detection algorithms for incrementally formed sheet metal parts, *T Nonferr Metal Soc*, 22 (2012) S315-S322.
- [91] A.K. Behera, H. Vanhove, B. Lauwers, J.R. Dufloy, Accuracy Improvement in Single Point Incremental Forming Through Systematic Study of Feature Interactions, *Key Eng Mater*, 473 (2011) 881-888.
- [92] R. Malhotra, J. Cao, F. Ren, V. Kiridena, Z.C. Xia, N.V. Reddy, Improvement of Geometric Accuracy in Incremental Forming by Using a Squeezing Toolpath Strategy With Two Forming Tools, *J Manuf Sci E-T Asme*, 133 (2011).
- [93] R. Malhotra, N.V. Reddy, J.A. Cao, Automatic 3D Spiral Toolpath Generation for Single Point Incremental Forming, *J Manuf Sci E-T Asme*, 132 (2010).
- [94] M. Azaouzi, N. Lebaal, Tool path optimization for single point incremental sheet forming using response surface method, *Simulation Modelling Practice and Theory*, 24 (2012) 49-58.
- [95] J. Dufloy, H. Vanhove, J. Verbert, J. Gu, I. Vasilakos, P. Eyckens, Twist revisited: Twist phenomena in single point incremental forming, *Cirp Ann-Manuf Techn*, 59 (2010) 307-310.
- [96] H. Vanhove, J. Verbert, J. Gu, I. Vasilakos, J. Dufloy, An experimental study of twist phenomena in single point incremental forming, *Int J Mater Form*, 3 (2010) 975-978.
- [97] R. Malhotra, J. Cao, M. Beltran, D. Xu, J. Magargee, V. Kiridena, Z.C. Xia, Accumulative-DSIF strategy for enhancing process capabilities in incremental forming, *Cirp Ann-Manuf Techn*, 61 (2012) 251-254.
- [98] M. Mirnia, B.M. Dariani, H. Vanhove, J. Dufloy, Thickness improvement in single point incremental forming deduced by sequential limit analysis, *Int J Adv Manuf Technol*, 70 (2014) 2029-2041.
- [99] M. Mirnia, B.M. Dariani, H. Vanhove, J. Dufloy, An investigation into thickness distribution in single point incremental forming using sequential limit analysis, *Int J Mater Form*, 7 (2014) 469-477.
- [100] Z. Liu, Y. Li, P.A. Meehan, Vertical wall formation and material flow control for incremental sheet forming by revisiting multistage deformation path strategies, *Materials and manufacturing processes*, 28 (2013) 562-571.
- [101] T. Cao, B. Lu, D. Xu, H. Zhang, J. Chen, H. Long, J. Cao, An efficient method for thickness prediction in multi-pass incremental sheet forming, *Int J Adv Manuf Technol*, 77 (2015) 469-483.
- [102] D. Xu, R. Malhotra, N.V. Reddy, J. Chen, J. Cao, Analytical prediction of stepped feature generation in multi-pass single point incremental forming, *Journal of Manufacturing Processes*, 14 (2012) 487-494.
- [103] R. Malhotra, A. Bhattacharya, A. Kumar, N. Reddy, J. Cao, A new methodology for multi-pass single point incremental forming with mixed toolpaths, *Cirp Ann-Manuf Techn*, 60 (2011) 323-326.
- [104] H. Vanhove, J. Gu, H. Sol, J. Dufloy, Process Window Extension for Incremental Forming through Optimal Work Plane Rotation, in: 10th anniversary of the International Conference on Technology of Plasticity, Aachen, Germany, 2011. 508-512
- [105] D. Xu, B. Lu, T. Cao, H. Zhang, J. Chen, H. Long, J. Cao, Enhancement of process capabilities in electrically-assisted double sided incremental forming, *Materials & Design*, 92 (2016) 268-280.

- [106] G. Ambrogio, L. Filice, G. Manco, Warm incremental forming of magnesium alloy AZ31, *Cirp Ann-Manuf Techn*, 57 (2008) 257-260.
- [107] A. Göttmann, M. Korinth, V. Schäfer, B.T. Araghi, M. Bambach, G. Hirt, Manufacturing of Individualized Cranial Implants Using Two Point Incremental Sheet Metal Forming, in: G. Schuh, R. Neugebauer, E. Uhlmann (Eds.) *Future Trends in Production Engineering*, Springer Berlin Heidelberg, 2013, pp. 287-295.
- [108] G. Fan, F. Sun, X. Meng, L. Gao, G. Tong, Electric hot incremental forming of Ti-6Al-4V titanium sheet, *Int J Adv Manuf Technol*, 49 (2010) 941-947.
- [109] G.Q. Fan, L. Gao, G. Hussain, Z.L. Wu, Electric hot incremental forming: A novel technique, *Int J Mach Tool Manu*, 48 (2008) 1688-1692.
- [110] G. Ambrogio, L. Filice, F. Gagliardi, Formability of lightweight alloys by hot incremental sheet forming, *Materials & Design*, 34 (2012) 501-508.
- [111] G. Palumbo, M. Brandizzi, Experimental investigations on the single point incremental forming of a titanium alloy component combining static heating with high tool rotation speed, *Materials & Design*, 40 (2012) 43-51.
- [112] D. Xu, B. Lu, T. Cao, J. Chen, H. Long, J. Cao, A comparative study on process potentials for frictional stir-and electric hot-assisted incremental sheet forming, *Procedia Engineering*, 81 (2014) 2324-2329.
- [113] Y. Ji, J. Park, Formability of magnesium AZ31 sheet in the incremental forming at warm temperature, *Journal of materials processing technology*, 201 (2008) 354-358.
- [114] A. Göttmann, D. Bailly, G. Bergweiler, M. Bambach, J. Stollenwerk, G. Hirt, P. Loosen, A novel approach for temperature control in ISF supported by laser and resistance heating, *Int J Adv Manuf Technol*, 67 (2013) 2195-2205.
- [115] M. Otsu, H. Matsuo, M. Matsuda, K. Takashima, Friction stir incremental forming of aluminum alloy sheets, *Steel Research International*, 81 (2010) 942-945.
- [116] D. Xu, W. Wu, R. Malhotra, J. Chen, B. Lu, J. Cao, Mechanism investigation for the influence of tool rotation and laser surface texturing (LST) on formability in single point incremental forming, *International Journal of Machine Tools and Manufacture*, 73 (2013) 37-46.
- [117] N.T. Nam, Hot incremental forming of magnesium and aluminum alloy sheets by using direct heating system, *Proceedings of the Institution of Mechanical Engineers, Part B: Journal of Engineering Manufacture*, 227 (2013) 1099-1110.
- [118] X. Cui, J. Mo, J. Li, J. Zhao, Y. Zhu, L. Huang, Z. Li, K. Zhong, Electromagnetic incremental forming (EMIF): a novel aluminum alloy sheet and tube forming technology, *Journal of Materials Processing Technology*, 214 (2014) 409-427.
- [119] M. Vahdati, R. Mahdavejad, S. Amini, Investigation of the ultrasonic vibration effect in incremental sheet metal forming process, *Proceedings of the Institution of Mechanical Engineers, Part B: Journal of Engineering Manufacture*, (2015) 0954405415578579.
- [120] S. Amini, A. Hosseinpour Gollo, H. Paktinat, An investigation of conventional and ultrasonic-assisted incremental forming of annealed AA1050 sheet, *Int J Adv Manuf Technol*, (2016) 1-10.
- [121] A.K. Behera, B. Lauwers, J.R. Dufloy, Tool path Generation for Single Point Incremental Forming using Intelligent Sequencing and Multi-step Mesh Morphing Techniques, *Int J Mater Form*, 8 (2013) 517-532.
- [122] S. Dejardin, S. Thibaud, J. Gelin, Finite element analysis and experimental investigations for improving precision in single point incremental sheet forming process, *Int J Mater Form*, 1 (2008) 121-124.
- [123] A. Hadoush, A. van den Boogaard, Efficient implicit simulation of incremental sheet forming, *International journal for numerical methods in engineering*, 90 (2012) 597-612.
- [124] S. He, A. Van Bael, P. Van Houtte, J.R. Dufloy, A. Szekeres, C. Henrard, A.M. Habraken, Finite element modeling of incremental forming of aluminum sheets, in: *Advanced Materials Research, Trans Tech Publ*, 2005, pp. 525-532.
- [125] C.F. Guzmán, J. Gu, J. Dufloy, H. Vanhove, P. Flores, A.M. Habraken, Study of the geometrical inaccuracy on a SPIF two-slope pyramid by finite element simulations, *International Journal of Solids and Structures*, 49 (2012) 3594-3604.
- [126] J. Verbert, J.R. Dufloy, B. Lauwers, Feature based approach for increasing the accuracy of the SPIF process, *Key Eng Mat*, 344 (2007) 527-534.
- [127] G. Hirt, J. Ames, M. Bambach, R. Kopp, Forming strategies and process modelling for CNC incremental sheet forming, *Cirp Ann-Manuf Techn*, 53 (2004) 203-206.
- [128] H. Meier, S. Reese, Y. Kiliçlar, R. Laurischkat, Increase of the dimensional accuracy of sheet metal parts utilizing a model-based path planning for robot-based incremental forming, in: *Process Machine Interactions*, Springer, 2013, pp. 459-473.
- [129] A. Mohammadi, H. Vanhove, A.K. Behera, A. Van Bael, J.R. Dufloy, In-Process Hardening in Laser Supported Incremental Sheet Metal Forming, *Key Eng Mater*, 504-506 (2012) 827-832.
- [130] A. Fiorentino, G. Feriti, C. Giardini, E. Ceretti, Part precision improvement in incremental sheet forming of not axisymmetric parts using an artificial cognitive system, *Journal of Manufacturing Systems*, 35 (2015) 215-222.
- [131] M.S. Khan, F. Coenen, C. Dixon, S. El-Salhi, M. Penalva, A. Rivero, An intelligent process model: predicting springback in single point incremental forming, *Int J Adv Manuf Technol*, 76 (2015) 2071-2082.
- [132] S. El Salhi, F. Coenen, C. Dixon, M.S. Khan, Predicting "springback" using 3D surface representation techniques: A case study in sheet metal forming, *Expert Systems with Applications*, 42 (2015) 79-93.
- [133] A.K. Behera, H. Ou, Effect of stress relieving heat treatment on surface topography and dimensional accuracy of incrementally formed grade 1 titanium sheet parts, *Int J Adv Manuf Technol*, 87 (9) (2016), pp. 3233-3248
- [134] M. Bambach, G. Hirt, Performance assessment of element formulations and constitutive laws for the simulation of incremental sheet forming (ISF), in: *VIII International Conference on Computational Plasticity*, 2005.
- [135] S. He, A. Van Bael, P. Van Houtte, Y. Tunckol, J. Dufloy, C. Henrard, C. Bouffieux, A. Habraken, Effect of FEM choices in the modelling of incremental forming of aluminium sheets, *8th ESAFORM Conference on Material Forming*, The publishing House of the Romanian Academy, 2005.
- [136] C. Bouffieux, P. Eyckens, C. Henrard, R. Aerens, A. Van Bael, H. Sol, J. Dufloy, A. Habraken, Identification of material parameters to predict Single Point Incremental Forming forces, *Int J Mater Form*, 1 (2008) 1147-1150.
- [137] C. Bouffieux, C. Henrard, P. Eyckens, R. Aerens, A. Van Bael, H. Sol, J. Dufloy, A. Habraken, Comparison of the tests chosen for material parameter identification to predict single point incremental forming forces, in: *International Conference of International Deep Drawing Research Group (IDDRG 2008)*, 2008.
- [138] C. Bouffieux, P. Pouteau, L. Duchene, H. Vanhove, J. Dufloy, A. Habraken, Material data identification to model the single point incremental forming process, *Int J Mater Form*, 3 (2010) 979-982.
- [139] M. Bambach, M. Cannamela, M. Azaouzi, G. Hirt, J. Batoz, Computer-aided tool path optimization for single point incremental sheet forming, in: *Advanced methods in material forming*, Springer, 2007, pp. 233-250.
- [140] M. Yamashita, M. Gotoh, S.-Y. Atsumi, Numerical simulation of incremental forming of sheet metal, *Journal of materials processing technology*, 199 (2008) 163-172.
- [141] J. Sena, R. Alves de Sousa, R. Valente, On the use of EAS solid-shell formulations in the numerical simulation of incremental forming processes, *Engineering Computations*, 28 (2011) 287-313.
- [142] J.I.V. Sena, C.F. Guzmán, L. Duchêne, A.M. Habraken, A.K. Behera, J. Dufloy, R.A.F. Valente, R.J.A. Sousa, Simulation of a two-slope pyramid made by SPIF using an adaptive remeshing method with solid-shell finite element, *Int J Mater Form*, 9 (2015) 383-394.
- [143] A. Delamézière, Y. Yu, C. Robert, L.B. Ayed, M. Nouari, J. Batoz, Numerical Simulation of Incremental Sheet Forming by Simplified Approach, in: *International Conference on Advances in Materials and Processing Technologies (AMPT2010)*, AIP Publishing, 2011, pp. 619-624.

- [144] G. Sebastiani, A. Brosius, A. Tekkaya, W. Homberg, M. Kleiner, Decoupled simulation method for incremental sheet metal forming, in: *Materials Processing and Design: Modeling, Simulation and Applications; Part Two(AIP Conference Proceedings Volume 908)*, 2007, pp. 1501-1506.
- [145] A.M.d.H. Hadoush, Efficient simulation and process mechanics of incremental sheet forming, PhD Thesis, University of Twente, 2010.
- [146] O.C. Zienkiewicz, R.L. Taylor, *The finite element method for solid and structural mechanics*, Butterworth-heinemann, 2005.
- [147] G. Ingarao, G. Ambrogio, F. Gagliardi, R. Di Lorenzo, A sustainability point of view on sheet metal forming operations: material wasting and energy consumption in incremental forming and stamping processes, *Journal of Cleaner Production*, 29 (2012) 255-268.
- [148] O. Anghinelli, G. Ambrogio, R. Di Lorenzo, G. Ingarao, Environmental Costs of Single Point Incremental Forming, *Steel Research Int.*, (2011) 525-530.
- [149] Y. Li, H. Lu, W.J. Daniel, P.A. Meehan, Investigation and optimization of deformation energy and geometric accuracy in the incremental sheet forming process using response surface methodology, *Int J Adv Manuf Technol.*, (2015) 1-15.
- [150] K. Branker, D. Adams, J. Jeswiet, Initial analysis of cost, energy and carbon dioxide emissions in single point incremental forming—producing an aluminium hat, *International Journal of Sustainable Engineering*, 5 (2012) 188-198.
- [151] M. Dittrich, T. Gutowski, J. Cao, J. Roth, Z. Xia, V. Kiridena, F. Ren, H. Henning, Exergy analysis of incremental sheet forming, *Production Engineering*, 6 (2012) 169-177.
- [152] I. Bagudanch, M. Garcia-Romeu, I. Ferrer, J. Lupiañez, The effect of process parameters on the energy consumption in Single Point Incremental Forming, *Procedia Engineering*, 63 (2013) 346-353.
- [153] G. Ingarao, K. Kellens, A.K. Behera, H. Vanhove, G. Ambrogio, J.R. Dufloy, Electric energy consumption analysis of SPIF processes, *Key Engineering Materials*, 549 (2013) 547-554.
- [154] G. Ingarao, H. Vanhove, K. Kellens, J.R. Dufloy, A comprehensive analysis of electric energy consumption of single point incremental forming processes, *Journal of Cleaner Production*, 67 (2014) 173-186.
- [155] G. Ambrogio, L. Filice, F. Gagliardi, Improving industrial suitability of incremental sheet forming process, *Int J Adv Manuf Technol.*, 58 (2012) 941-947.
- [156] G. Ambrogio, G. Ingarao, F. Gagliardi, R. Di Lorenzo, Analysis of energy efficiency of different setups able to perform single point incremental forming (SPIF) processes, *Procedia CIRP*, 15 (2014) 111-116.
- [157] I. Bagudanch, M. Garcia-Romeu, M. Sabater, Incremental forming of polymers: process parameters selection from the perspective of electric energy consumption and cost, *Journal of Cleaner Production*, 112 (2015) 1013-1024.
- [158] I. Bagudanch, M. Vives-Mestres, M. Sabater, M.L. Garcia-Romeu, Polymer incremental sheet forming process: Temperature analysis using response surface methodology, *Materials and Manufacturing Processes*, 32 (2017) 44-53.
- [159] J. Allwood, G. King, J. Dufloy, A structured search for applications of the incremental sheet-forming process by product segmentation, *Proceedings of the Institution of Mechanical Engineers, Part B: Journal of Engineering Manufacture*, 219 (2005) 239-244.
- [160] G. Ambrogio, L. De Napoli, L. Filice, F. Gagliardi, M. Muzzupappa, Application of Incremental Forming process for high customised medical product manufacturing, *Journal of Materials Processing Technology*, 162-163 (2005) 156-162.
- [161] J. Dufloy, B. Lauwers, J. Verbert, F. Gelaude, Y. Tunckol, Medical application of single point incremental forming: cranial plate manufacturing, in: *Proc. 2nd Internat. Conf. on Advanced Research in Virtual and Rapid Prototyping, VRAP, Leiria, 2005*, pp. 161-166.
- [162] V. Oleksik, A. Pascu, C. Deac, R. Fleaca, M. Roman, O. Bologa, The influence of geometrical parameters on the incremental forming process for knee implants analyzed by numerical simulation, *NUMIFORM 2010*, (2010) 1208-1215.
- [163] A. Fiorentino, G.P. Marena, R. Marzi, E. Ceretti, D.T. Kemmoku, J.V.L. Silva, Rapid Prototyping techniques for individualized medical prosthesis manufacturing, in: *Innovative Developments in Virtual and Physical Prototyping*, CRC Press, 2011, pp. 589-594.
- [164] A. Fiorentino, R. Marzi, E. Ceretti, Preliminary results on Ti incremental sheet forming (ISF) of biomedical devices: biocompatibility, surface finishing and treatment, *International Journal of Mechatronics and Manufacturing Systems*, 5 (2012) 36-45.
- [165] P.D. Eksteen, A.F. Van der Merwe, Incremental Sheet Forming (ISF) in the Manufacturing of Titanium Based Plate Implants in the Bio-Medical Sector, in: *Proceedings of the International Conference on Computers & Industrial Engineering (CIE 42)*, Cape Town, South Africa, 2012, pp. 569-575.
- [166] P.D.W. Eksteen, Development of incrementally formed patient-specific titanium knee prosthesis, Thesis (MScEng), Stellenbosch University, 2013.
- [167] J.R. Dufloy, A.K. Behera, H. Vanhove, L.S. Bertol, Manufacture of Accurate Titanium Cranio-Facial Implants with High Forming Angle Using Single Point Incremental Forming, *Key Eng Mater.*, 549 (2013) 223-230.
- [168] I. Bagudanch, L.M. Lozano-Sánchez, L. Puigpinós, M. Sabater, L.E. Elizalde, A. Elías-Zúñiga, M.L. Garcia-Romeu, Manufacturing of polymeric biocompatible cranial geometry by single point incremental forming, *Procedia Engineering*, 132 (2015) 267-273.
- [169] J. Allwood, A.N. Bramley, T. Ridgman, A. Mileham, A novel method for the rapid production of inexpensive dies and moulds with surfaces made by incremental sheet forming, *Proceedings of the Institution of Mechanical Engineers, Part B: Journal of Engineering Manufacture*, 220 (2006) 323-327.
- [170] R. Appermont, B. Van Mieghem, A. Van Bael, J. Bens, J. Ivens, H. Vanhove, A.K. Behera, J. Dufloy, Sheet-metal based molds for low-pressure processing of thermoplastics, in: *Proceedings of the 5th Bi-Annual PMI Conference*, 2012, pp. 383-388.
- [171] A. Governale, A. Lo Franco, A. Panzeca, L. Fratini, F. Micari, Incremental forming process for the accomplishment of automotive details, in: *Key Engineering Materials*, 344 (2007) 559-566.
- [172] L. Junchao, S. Sunjian, W. Bin, A multipass incremental sheet forming strategy of a car taillight bracket, *Int J Adv Manuf Technol.*, 69 (2013) 2229-2236.
- [173] M.L. Garcia-Romeu, I. Bagudanch, L.M. Lozano-Sánchez, O. Martínez-Romero, A. Elías-Zúñiga, L.E. Elizalde, On the manufacture of biomedical devices based on nano-polymer composites by single point incremental forming, in: C.A. Rodriguez (Ed.) *2nd International Conference on Design and PROCesses for MEDical Devices (PROMED 2014)*, Monterrey, Mexico, 2014, pp. 49-52.
- [174] I. Bagudanch, M.L. Garcia-Romeu, I. Ferrer, Manufacturing of thermoplastic cranial prosthesis by incremental sheet forming, in: C.A. Rodriguez (Ed.) *2nd International Conference on Design and PROCesses for MEDical Devices (PROMED 2014)*, Monterrey, Mexico, 2014, pp. 95-98.
- [175] G. Centeno, D. Morales-Palma, I. Bagudanch, A.J. Martínez-Donaire, M.L. García-Romeu, C. Vallengano, Experimental strain analysis on the manufacturing of polymer cranial prosthesis by single-point incremental forming, in: I.B. Corral, J.M. Canela (Eds.) *6th Manufacturing Engineering Society International Conference (MESIC 2015)*, Barcelona, Spain, 2015.
- [176] J. Liu, W. Liu, W. Xue, Forming limit diagram prediction of AA5052/polyethylene/AA5052 sandwich sheets, *Materials & Design*, 46 (2013) 112-120.
- [177] H. Yao, C.-C. Chen, S.-D. Liu, K. Li, C. Du, L. Zhang, Laminated steel forming modeling techniques and experimental verifications, *SAE Technical Paper*, 2003.
- [178] University of Cambridge, Incremental Sheet Forming, Available online at: <http://www.lcmp.eng.cam.ac.uk/wellformed/incremental-sheet-forming>, 2009, Last accessed 28th February, 2017
- [179] A.J.B. Lozano, G.J.P. Bermudez, F.A.B. Correa, Comparative Analysis between the SPIF and DPIF Variants for Die-less Forming Process for an Automotive Workpiece, *INGE CUC*, 11 (2015) 68-73.

- [180] Ford Motor Company, Ford develops advanced technology to revolutionize prototyping, personalization, low-volume production, Available online at: <https://media.ford.com/content/fordmedia/fna/us/en/news/2013/07/03/ford-develops-advanced-technology-to-revolutionize-prototyping-.html>, 2013, Last accessed 28th February, 2017
- [181] Y. Wang, W. Peng, A deformation analysis and experimental study for a novel full kinematic incremental forming, *Australian Journal of Mechanical Engineering*, (2015) 1-9.
- [182] T. McAnulty, J. Jeswiet, M. Doolan, Formability in single point incremental forming: A comparative analysis of the state of the art, *CIRP Journal of Manufacturing Science and Technology*, (2016).
- [183] L. Thyssen, P. Seim, D.D. Störkle, B. Kuhlenkötter, On the increase of geometric accuracy with the help of stiffening elements for robot-based incremental sheet metal forming, *AIP Conference Proceedings*, 1769 (2016) 070008.
- [184] I. Paniti, Adaptation of Incremental Sheet Forming into cloud manufacturing, *CIRP Journal of Manufacturing Science and Technology*, 7 (2014) 185-190.